Vibration Institute 34th Annual Meeting, June 22-26, 2010 Oak Brook, Illinois

DYNAMIC STABILITY and WHIRL MOTION of LARGE DIESEL ENGINE TURBOCHARGERS in FLOATING BUSH and MULTI-LOBED BEARINGS

Edgar J. Gunter, Ph.D.
RODYN ***Vibration Analysis, Inc.***
Professor Emeritus Mechanical and Aerospace Engineering
Former Director, Rotor Dynamics Laboratory, Univ. Of Virginia
Fellow ASME
DrGunter@aol.com

Wen Jeng Chen, Ph.D.
Eigen Technologies, Inc.
Fellow ASME
Dyrobes@apex.net

Abstract:

This paper deals with the stability and nonlinear dynamical analysis of a class of turbocharger used on locomotives and marine diesel engines. These larger sized turbochargers operate at 30,000 RPM and use floating ring bearings. The floating ring bearing is very common for use in the smaller highspeed automotive engines. The use of floating ring bearings for the heavier turbochargers can encounter a number of difficulties which can lead to catastrophic failure of the impeller and shaft, depending upon operating conditions and clearance values of the bearings. All turbochargers mounted in floating ring bearings are inherently unstable with limit cycle whirling. The whirl orbits are controlled by the nonlinear bearing forces generated in the inner and outer fluid films of the bearings. Depending upon the floating ring bearing clearances, a sufficiently high whirl motion can occur, causing the compressor impeller to rub, leading to impeller and shaft failure. A very tight internal compressor bearing ring clearance may cause the bushing to freeze to the shaft. When this occurs the bushing acts as a large clearance journal bearing and is violently unstable. The ensuing large amplitude whirl motion leads to rapid turbocharger failure. Dynamical models are presented to show the nonlinear behavior of the turbocharger and the magnitudes of the limit cycle whirl motion with both the floating bush bearing and various multi-lobed bearing designs. Attempts to make a multilobed bearing out of a floating bush bearing by adding axial grooves is not effective and may actually lead to larger whirl orbits. Improvements in turbocharger reliability with floating bush bearings may be obtained by the use of closely controlled bearing ring clearances, use of a synthetic lubricant, secondary turbocharger oil filtration, turbocharger overspeed controls, and increased radial clearances in the turbocharger inducer and compressor sections. Finally, a superior bearing design is presented using a 3 lobed bearing design which improves the stability characteristics and reduces the nonsynchronous whirl amplitudes.

Keywords: Floating bush bearings; limit cycle motion; multi-lobed bearings; nonlinear transient response; rotor stability; self-excited whirling; turbochargers

Introduction:

The turbochargers used for the large stationary and marine diesel engines are considerably larger than the typical turbochargers used in automotive engines. The diesel engine turbocharger under consideration is shown in Figure 1.

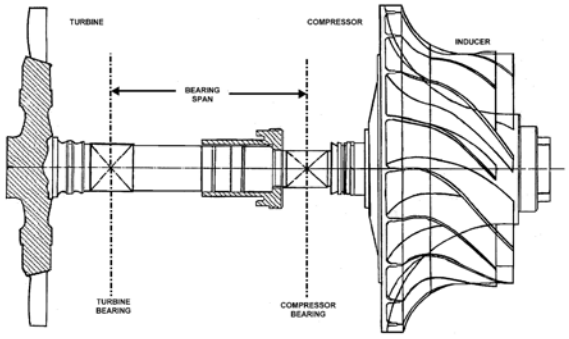

Fig. 1 Diesel Engine Turbocharger

These turbochargers operate at a speed of approximately 30,000 RPM, as compared to over 100,000 RPM for the automotive turbochargers. The typical turbocharger design is a double overhung turbo-rotor with a steel turbine wheel of high temperature alloy and an attached aluminum compressor wheel. The typical type of bearings used for the smaller high-speed automotive turbochargers is the floating ring bearing. The concept of the floating ring bearing was developed in the 1930s. The original concept was to reduce horsepower losses. A plain journal bearing, for example, will not operate satisfactorily in either the smaller turbochargers operating at 100,000 RPM or the much larger diesel engine turbochargers with an operational speed of only 30,000 RPM. The reason for this is due to the inherent self-excited whirl instability encountered with a fixed plain journal bearing. At higher speeds, the rotor will go into a subsynchronous whirl motion. Continued operation with a plain journal bearing at high speed will result in excessive bearing wear followed by total rotor failure.

With the floating ring bearing, for example, as shown in Figure 12, the journal bearing is not fixed but is a ring which is free to float on the shaft. The ring rotates at a fraction of the shaft running speed from a theoretical maximum of 50% to as low as 15% of running speed. The ring speed is controlled by the viscosity of the inner and outer oil films and the clearances of the inner and outer bearings. The inner ring clearance of the ring is kept at a much tighter clearance than the outer ring. This causes more friction losses in the inner clearance, resulting in higher temperatures and lower oil viscosity.

Although the floating ring bearing itself is unstable from a linearized standpoint, the rotor motion will form a limit cycle whirl motion due to the nonlinear bearing forces. This is referred to as subsynchronous whirling with double overhung turbochargers. The turbocharger will precess at a fraction of running speed. Normally, the whirl motion encountered is a conical whirling motion. Under properly designed clearance ratios for the floating ring bearing, the small turbochargers may run at high speed with controlled limit cycle whirling.

Although the concept of the floating ring bearing is quite simple, the analysis of the dynamical behavior of a turbocharger in a floating ring is exceedingly difficult. This is due to the nonlinear nature of the fluid film and the requirement of the numerical integration of the equations of motion. The advantage of the floating ring bearing is in its simplicity and cost of manufacture. Although the floating ring bearing is simple to manufacture and is low in cost, it is not recommended for the larger diesel engine turbochargers. A bearing superior to the floating bush bearing is the multilobed or specifically the 3 lobed bearing. This bearing is more expensive to manufacture but due to the initial cost of these larger turbochargers, the extra cost is warranted. It will be seen that the 3 lobed bearing has greater stability.

Description of Diesel Engine Turbocharger:

The left section as shown in Fig. 1 represents the steel turbine wheel. To the right is attached the aluminum compressor wheel with the inducer section. The inducer section is separate from the compressor wheel. Typical turbochargers are double overhung rotors. That is, the bearings are inboard of the turbocharger compressor and turbine wheels. The left bearing represents the turbine-end bearing, and the right end is the compressor-end bearing. Adjacent to the compressor bearing is the thrust bearing. It should be noted that the turbine-end bearing is larger than the compressor-end bearing. The reason for this is for ease of assembly and disassembly for field maintenance.

Figure 2 represents a cutaway of the diesel-engine turbocharger. This figure is of interest as it shows the construction and method of attachment of the compressor and inducer wheels. The steel shaft extends under the compressor and inducer wheels. The compressor wheels are attached to the wheel shaft by means of a sleeve and bolt arrangement. There is an end cap, or bell, which maintains the compressor and inducer wheels. In Figure 1, the compressor wheel assembly appears to be fairly rigidly attached to the shaft. In reality, because of the extension of the steel shaft and the sleeve, the overhang of the compressor section is fairly flexible.

Design Considerations for the Turbocharger:

The principle design consideration for the turbocharger is primarily with the aerodynamic performance of the compressor wheel and the design of the turbine for the power required to drive the compressor. The aerodynamics of the compressor design are indeed quite elaborate, as the compressor design is quite sophisticated in order to meet the head requirements for the system. The turbocharger compressor wheel is always an open-bladed radial centrifugal compressor design with a backward sweep. The backward sweep of the blades is to generate a larger Q/N flow region. In order not to starve the inlet of the compressor wheel, there are 10 splitter vanes in addition to the 10 larger impeller vanes.

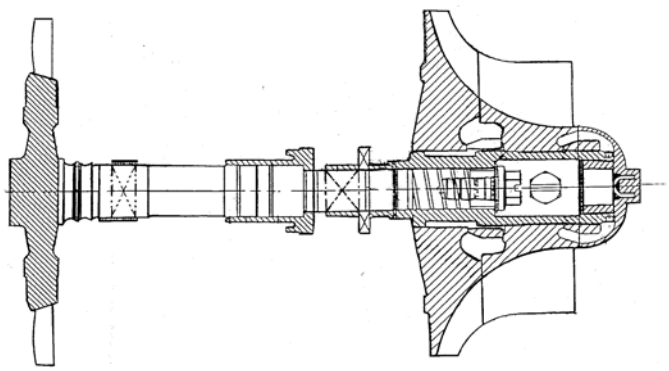

Fig 2 Turbocharger Cross Section

Small auto engine turbochargers operate at speeds exceeding 100,000 RPM. The design speed of this particular type of the turbocharger is 30,000 RPM. The primary consideration for the smaller turbochargers is cost, as the smaller ones may cost only several hundred dollars. These larger turbochargers may exceed $70,000 in cost. The cost of repair and replacement of these turbochargers therefore can represent a considerable outlay of funds. The second major design consideration for the turbocharger is the centrifugal stresses in the turbine, and particularly the compressor wheel. These compressors are designed such that they are well below the burst speed. A third major consideration for the design of the turbocharger is ease of assembly and disassembly. The steel alloy turbine wheel is usually friction welded to the steel shaft. The aluminum impeller wheels are attached to the shaft, as previously mentioned, by the sleeve.

Since the compressor wheel is assembled and bolted on to the steel shaft, this results in a compressor bearing design which is smaller than the turbine bearing.

Compressor and inducer wheel clearances as such are required to be close to line to line contact. At the operating speed of 30,000 RPM, the centrifugal expansion of the compressor wheel assembly, therefore, does not provide a great deal of stiffening to the steel shaft and the extension sleeve. The major stiffness of the assembly is controlled by the steel shaft supporting the compressor wheel and inducer.

The final consideration for the design of these high-speed turbochargers is the bearing type to be employed with the turbocharger. With the smaller turbochargers, the floating ring bearing is commonly used. With the smaller automobile type turbochargers, where cost is a great consideration, the floating bush bearing has found to be satisfactory provided that proper clearances of the inner and outer ring are maintained. This type of bearing is also currently being used in this particular class of turbocharger.

The problem with the floating ring bushing design is that at high speeds, the turbocharger is inherently unstable. That is, the turbocharger exhibits self-excited whirl motion in which the turbocharger is precessing or whirling at a lower frequency. This is referred to as nonsynchronous precession. The predominate whirl mode is usually a conical motion of the rotor. By properly controlling the ring inner and outer clearances , a bounded finite limit cycle orbit or motion can be obtained. In order to keep this limit cycle motion within bounds, the inner clearance must be very tight, leading to high bearing temperatures and other operating problems associated with tight bearing clearances.

The floating bush bearing operates by spinning at a fraction of the rotor speed. The typical precession rate of the ring speed may be from 15-30% of shaft speed. The outer ring clearance is normally several times larger then the clearance of the outer ring. Theoretical ring speed can go as high as 50%, although this is never achieved in practice. The maximum ring speed is limited by the higher temperatures generated in the inner ring. By properly controlling the ring inner and outer clearances, a bounded finite limit cycle orbit or motion can be obtained.
The mechanism of the outer ring acts as a type of crude squeeze-film damper to generate nonlinear forces to cause a limit cycle whirl motion. This bearing type, which is well suited for the smaller turbochargers because of cost consideration, is not an ideal bearing for the larger, more expensive turbochargers. The larger turbochargers, which weigh approximately 44 lbs, may operate with large limit cycle motions, even with properly controlled clearances. In addition to the self-excited whirl motion inherent in the floating bushings themselves, there are additional aerodynamic forces that creates self-excited whirl motion in all compressors and turbines. This effect is referred to as the Alford effect. The Alford effect causes cross-coupled aerodynamics bearing forces to act on the compressor and turbine, which also promotes instability.

It will also be shown that the compressor bearing should be larger than the turbine bearing, since this bearing carries the higher bearing loads. The smaller compressor bearings are designed from the standpoint of the ease of assembly and disassembly. It will be seen that damage and failure are predominantly associated with the compressor-end bearings. Unfortunately, with most turbochargers, whether they be small or large, the bearing design is an approximation based on previous practice and experience. The engineering, until recently, has been limited because of the lack of rotor dynamics codes to compute the nonlinear fluid-film bearing forces and also the nonlinear time transient motion of the turbocharger.

These bearings usually are designed and perfected primarily based on experimental testing. Since the large diesel engine turbochargers cost an order of magnitude greater than the smaller automotive turbochargers, one can afford to design a more effective bearing system for the turbochargers, such as the multi-lobed bearing. The theory of these multi-lobed bearings is well established and has also been employed in other large diesel engine turbochargers.

It is now possible to combine the nonlinear fluid-film characteristics of either the floating-ring or the multi-lobed bearing with a nonlinear time transient analysis of the complete turbocharger to generate the magnitude of the limit cycle motion and bearing forces transmitted. At the time this class of turbocharger was designed, this type of technology was not generally available for commercial use.

Critical Speed Analysis:

Although the bearings for the turbocharger are highly nonlinear, it is of considerable value to perform a critical speed analysis of the turbocharger. By means of a critical speed analysis, one can determine the relative mode shapes and the energy distribution in each bearing and shaft for that particular mode.

Figure 3 represents a computer model of the turbocharger used for the critical speed analysis. The model contains 48 degrees-of-freedom and represents three levels of attachment. It should be noted that a computation of a built up rotor or multi-level rotor construction is difficult to perform using the transfer matrix method.

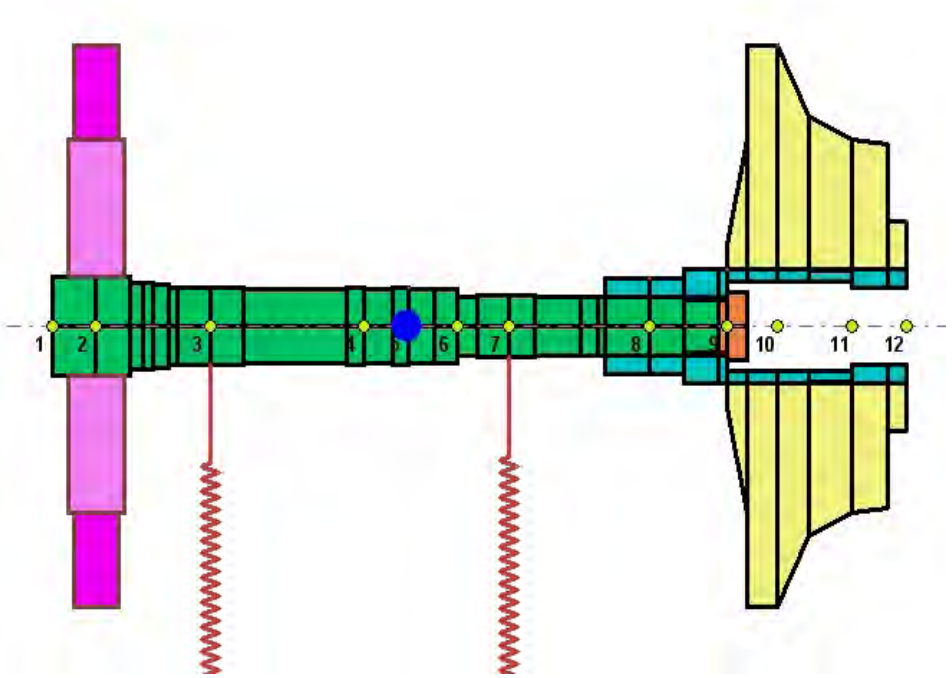

Fig 3 Critical Speed Model

Station 2 represents the turbine section. The turbine bearing is located at station 3 and the compressor bearing is located at station 7. The compressor and inducer sections are attached to a steel shaft which is in turn held to the main shaft by means of a bolt attachment. The circular dot near station 5 represents the center of gravity of the entire assembly.

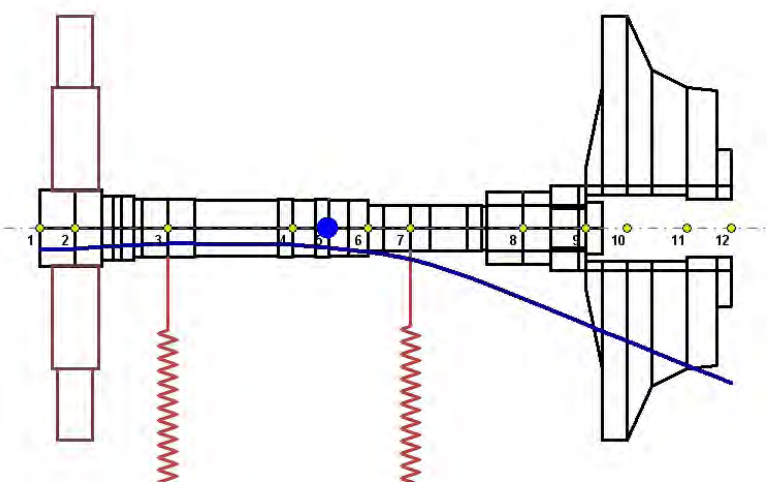

Fig. 4 Turbocharger Static Deflection

Figure 4 represents the static deflection of the rotor. The bearing loads on each bearing are also computed with this calculation. Note that since the center of gravity is closer to the compressor bearing, the compressor bearing carries a greater load than does the larger turbine bearing. The relative load on the turbine bearing is 15 lbs and it is approximately 30 lbs on the compressor bearing. Therefore, although the compressor bearing is smaller, it is carrying twice the static loading of the turbine bearing.

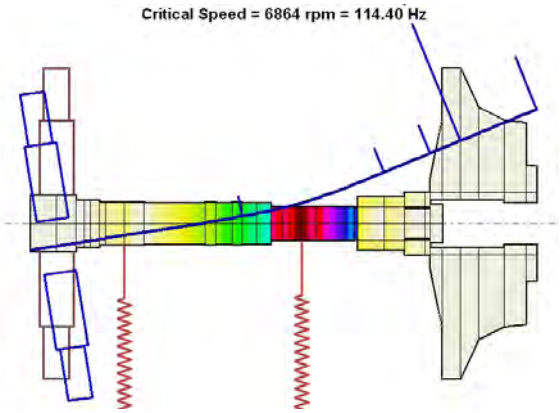

Fig. 5 1st Turbocharger Mode

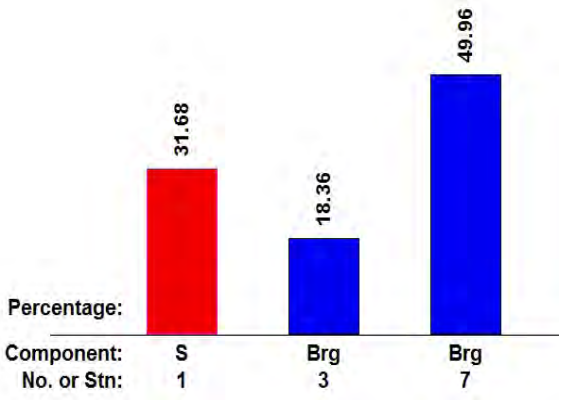

Fig. 6 1st Mode Shaft & Bearing Strain Energies

Fig. 5 represents the relative turbocharger 1st mode. This conical mode shape is typical with all double overhung rotors with inboard bearings. Note that the maximum motion is at the compressor inducer location.

Fig. 6 represents the relative strain energy in the shaft and bearings for the 1st mode. Note that 50% of the 1st mode strain energy is associated with the smaller compressor bearing. The maximum shaft strain energy for this mode is concentrated under the compressor bearing. This is the location in which failure has been experienced. Since the disks are outboard of the bearings, the lowest mode is a conical whirl mode. It will be seen that this mode is the easiest mode to excite for self-excited instability. Also, when the turbocharger becomes unstable and whirls in this conical mode, large amplitudes occur at the compressor and inducer section, making it very susceptible to rubs.

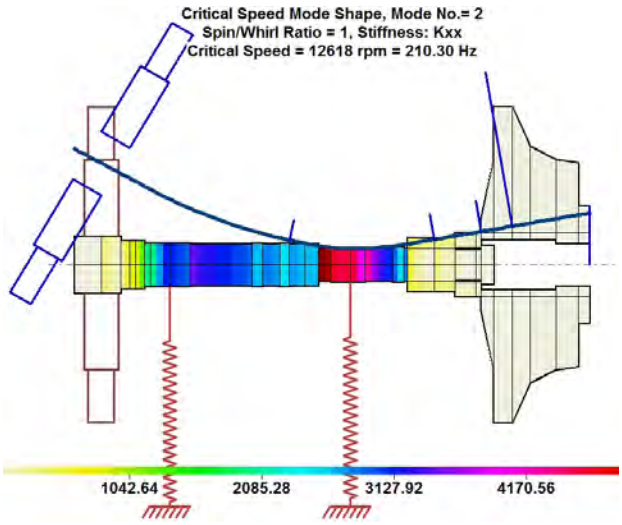

Fig. 7 2nd Turbocharger Mode

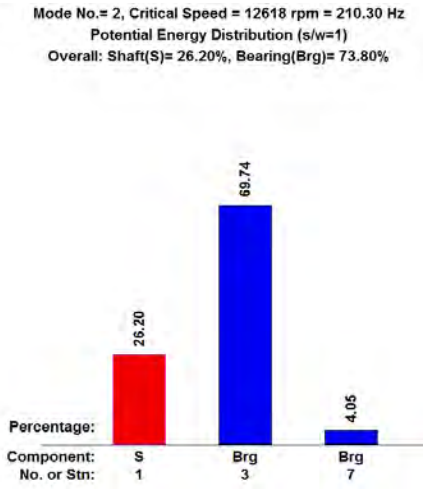

Fig. 8 2nd Mode Relative Shaft & Bearing Strain Energies

Figure 7 represents the second mode of the turbocharger. In this mode, the turbine and compressor are in phase. There is more bending strain energy in the shaft. The turbocharger may exhibit instability in the second mode, as well as the first. However, the higher, or cylindrical mode, is normally not as sensitive to unbalance or self-excited motion as the conical lower mode is. Figure 7 represents the strain energy distribution for the second mode. In this mode it is seen that there is a much higher strain energy distribution in the turbine-end bearing. The compressor end bearing has little influence on controlling this mode.

Fig. 9 represents the turbocharger 3rd mode. Under normal conditions, this mode should be above the operating speed with well designed bearings. This mode is shown to be at a speed of 54,000 RPM with the assumed linear bearings. With a loose connection of the compressor attachment section to the main shaft , this higher bending critical speed may be greatly reduced.

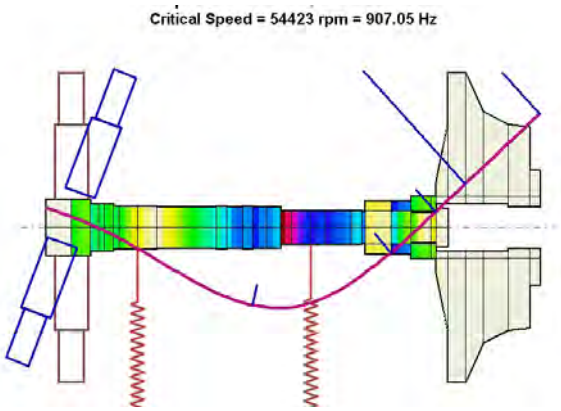

Fig. 9 Turbo 3rd Mode at 54,000 RPM

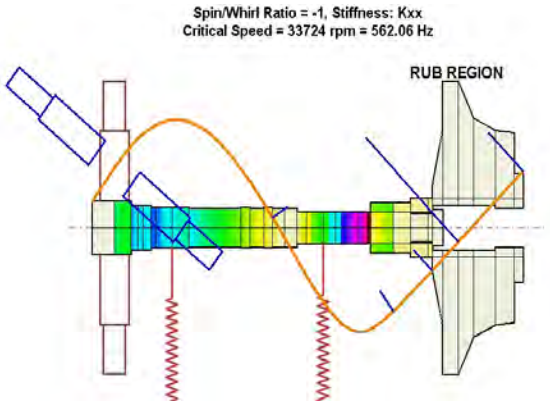

Fig. 10 Backward Mode at 33,700 RPM

Fig. 10 represents the 4th backward mode at 33,724 RPM. If the turbocharger should over speed and rub, then this mode could be excited causing a violent backward precession of the compressor wheel. Hence, any instances of rubbing on the inducer or compressor at operating speed could lead to the initiation of a violent sustained backward whirling causing failure.

Modeling of Turbocharger in Floating Bush Bearings:

The diesel engine turbocharger, including the floating bush fluid-film bearings, was modeled using the ***DyRoBeS*** rotor-bearing dynamics software. Figure 11 represents a cross-section of the turbocharger as modeled using the ***DyRoBeS*** software to include the floating bush bearings. The rotor is modeled with 11 finite element shaft elements which include 30 sub-elements. The rotor is actually modeled as a 3-bearing system. The bearings 1 and 2, at stations 3 and 7, represent the floating bush bearings.

The bearing station at station 10 is used to introduce the Alford type of aerodynamic cross-coupling forces acting on the compressor wheel. The complete system is represented by a total of 52 degrees-of-freedom for displacements and rotations. Note that the center of gravity of the turbo is closer to the compressor bearing. This causes the compressor bearing loads to be double the turbine bearing. Also shown on Figure 11 is a red arrow at station 10. This represents an applied unbalance. In addition to external forcing functions such as unbalance, one could also add shaft bow and disk skew as exciting forces. From a linearized stability standpoint the system would be characterized by 104 complex eigenvalues. Of these eigenvalues, only the lower modes are of interest.

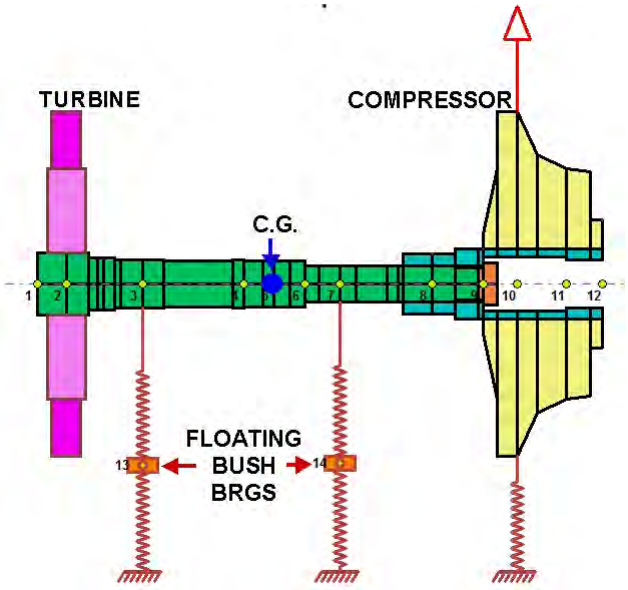

Fig. 11 *DYROBES* Turbo Model Including Floating Bush Bearings

Floating Bush Bearings:

A schematic of the floating bush bearings is shown in Fig. 12. The location of the floating bush bearings are at stations 13 and 14 as shown in Fig. 11. The masses of the rings are acting at stations 13 and 14.

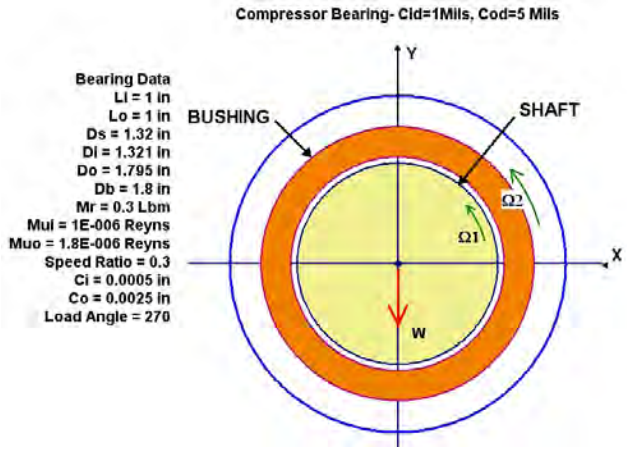

Fig. 12 Schematic of Floating Bush Bearing

In order to perform a time transient analysis, the equations of motion are integrated forward in time. It is required, therefore, to integrate 52 second order equations simultaneously while computing the nonlinear bearing fluid-film forces at each time increment. Some care has to be exhibited in generating the model in order to expedite the numerical time transient calculations and to ensure convergence of the solution. The numerical nonlinear time transient solution will be discussed in detail in a later section.

With this model, in addition to the time transient response, one may calculate the nonlinear synchronous unbalance response of the turbocharger system due to assumed values of unbalance acting on the compressor or turbine. In addition to the response caused by radial unbalance, the influence of shaft bow or disk skew may also be included.

It is apparent from looking at the critical speed mode shapes and energy distribution that the conical whirl mode is of greatest concern. The larger turbine bearing will have little influence on controlling this mode as the predominant strain energy is in the compressor bearing. Although the turbine bearing has a reduced strain energy as compared to the compressor bearing, paradoxically an increase in the turbine floating ring clearances will cause excessive conical motion leading to turbocharger failure. Therefore, we shall see later that the clearance specifications of the turbine floating bush bearing cannot be ignored.

Floating Bush Bearing Coefficients:

Although the behavior of the floating bush bearings are highly nonlinear, it is desirable to determine the linearized bearing coefficients in order to perform a complex damped eigenvalue analysis on the system. This is usually referred to as a stability analysis. The critical speed analysis is an undamped analysis which assumed circular synchronous precession. In this analysis, only one nominal bearing coefficient is assumed. In order to perform a stability analysis, the computation of 8 bearing coefficients are required for both the inner and outer surfaces of the floating bush bearing.

Table 1 represents some typical dimensions of the turbocharger floating bush bearings. It is seen that the turbine bearing is larger than the compressor bearing even though it is carrying a much lower load. Using these dimensions the bearing stiffness and damping coefficients may be computed for each bearing. These dimensions are used for the computation of the bearing coefficients for each ring.

Table 1 - Floating Bush Bearing Characteristics

	D_s	L_i	C_d	D_b	L_o	C_{od}	W
Compressor	**1.32**	**1.0**	**.001**	**1.80**	**1.0**	**.005**	**33**
Turbine	**1.70**	**1.0**	**.002**	**2.165**	**1.0**	**.005**	**11**

In Table 1 is shown the inner and outer clearances of the compressor and turbine end bushing bearings. Note that the specified diametral internal clearance of the compressor bushing is 1 mil. This is about one-third the thickness of a human hair. With this tight a clearance, the compressor bearing must be well supplied with oil as it will run hot. The outer ring clearances are 5 mils. The outer ring clearances are normally specified as larger then the inner ring clearances. The specified ranges of clearances permitted for both bearings is rather large. For example, the turbine bearing clearance is specified to be as large as 3.2 mils for the inner clearance and 10.5 mils for the outer ring clearance. It will be seen that these large values of specified permissible clearances is excessive and will lead to turbocharger failure.

Figure 13 represents the bearing pressure profile and stiffness and damping coefficients for the compressor end bearing. The inner and outer surfaces of the ring develop a very similar pressure profile except that the bearing coefficients generated from each pressure field are considerably different.

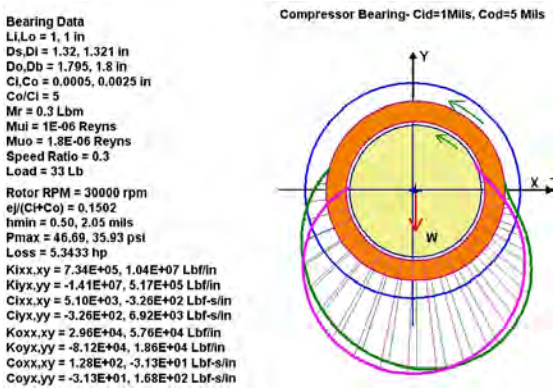

Fig. 13 Compressor Floating Bush Bearing Coefficients at 30,000 RPM

There are two assumptions that were made in the calculation of the floating bush bearing coefficients. The ring speed was computed to be around 0.3 and the oil viscosity of the inner ring is always assumed to be lower that the outer ring viscosity.

Tables 2 and 3 represent the bearing coefficients for the compressor and turbine bearings

Table 2

Compressor Bush Bearing Coefficients - 30,000 RPM

	K_{XX}	K_{XY}	K_{YX}	K_{YY}	C_{XX}	C_{XY}	C_{YX}	C_{YY}
Inner	**.733E6**	**10.4E6**	**-14.1E6**	**.52E6**	**5100**	**-326**	**-326**	**6920**
Outer	**30,000**	**58,000**	**-81,200**	**18,600**	**128**	**-31**	**-31**	**128**

In Tables 2 and 3, it is seen that the inner oil film stiffnesses are an order of magnitude higher then the bearing coefficients generated by the outer film. Note also that the inner ring bearing stiffness cross coupling coefficients are an order of magnitude greater than the direct bearing stiffness coefficients. The high cross coupling stiffness coefficients are the principle source of the cause of self excited nonsynchronous whirl motion.

TABLE 3

Turbine Bush Bearing Coefficients - 30,000 RPM

	K_{XX}	K_{XY}	K_{YX}	K_{YY}	C_{XX}	C_{XY}	C_{YX}	C_{YY}
Inner	**.63E6**	**15.0E6**	**-19.4E6**	**.57E6**	**7360**	**-300**	**-300**	**9500**
Outer	**11,100**	**69,000**	**-87,000**	**4810**	**150**	**-13**	**-13**	**184**

Stability of Turbocharger in Floating Ring Bearings:

Using the floating bush bearing coefficients, based on nominal clearances, as shown in Tables 2 and 3, a damped eigenvalue analyses may be performed to determine the relative stability of the turbocharger at the assumed operating speed of 30,000 RPM. By varying the turbine and compressor ring clearances, it may be determined which clearance values produce improved stability characteristics. In addition to the bearing coefficients, an additional aerodynamic cross-coupling excitation of 500 lb/in was assumed acting at the compressor location.

Based on the bearing characteristics, as shown in Table 2 and 3, the damped eigenvalues for the turbocharger were computed. Figure 14 represents the first forward mode of the turbocharger, and it is a conical motion with the maximum amplitude at the compressor. With the dimensions as specified in Table 1, the first conical mode is stable with a whirl frequency of 4814 CPM and a log decrement of 0.31.

In order to achieve this predicted stable motion based on linearized bearing coefficients, the inner ring clearance of the compressor bearing is a tight 1 mil clearance and the turbine diametral clearance is 2 mils. The outer ring clearance for both bearings is 5 mils. The conical mode shape is essentially a rigid body mode with the largest amplitude at the compressor and inducer location. The indicated subsynchronous whirl frequency is 4814 CPM.

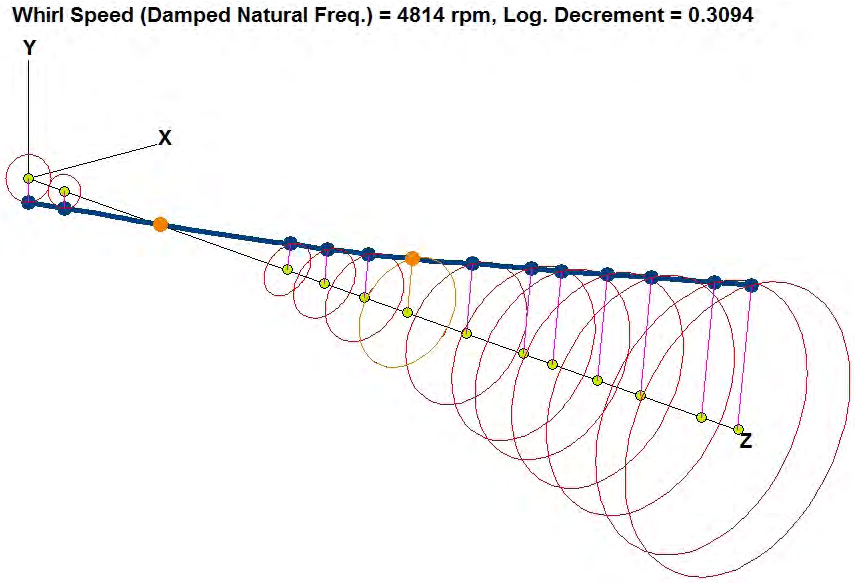

Fig. 14 Stable 1st Mode With Nominal Brg Clearances
Nf1 = 4814 CPM , Log Decrement δ = .31

The 1st conical mode is stable with the coefficients as listed in Tables 2 & 3. If, however, the turbine bearing ring clearances are increased from the nominal values of 2 mils for the inner clearance and 5 mils for the outer ring clearance to the stated maximum values of 3.2 mils internal and 10.5 mils external, then we have an unstable situation as shown in Fig. 15.

The increase in turbine bearing clearances causes an unstable whirling situation. Strict limits on the turbine bearing must be maintained to minimize self excited instability to occur. Hence a sloppy turbine bushing bearing is an invitation to turbocharger failure, even though no failure of the turbine bearing itself is ever experienced. Therefore, it appears that the maximum turbine bearing clearance values as specified by the manufacturer are not permissible, as this would induce turbocharger instability in the first conical mode.

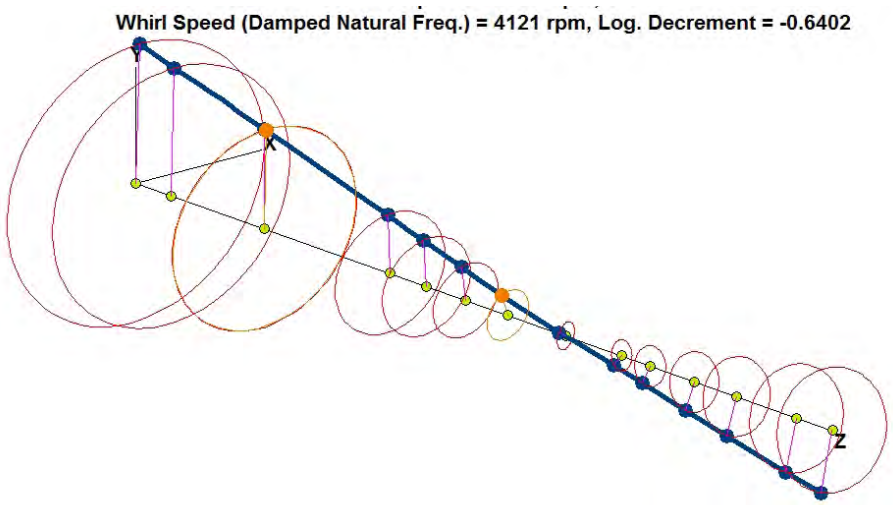

Fig. 15 Unstable 1st Mode With Maximum Turbine Bearing Clearances, Nf1 = 4121CPM , δ = - 0.64

Although the turbine bearing never experiences failure, it is imperative that this bearing clearance be kept tight in order to maintain proper stability. Instability in the higher cylindrical mode is also encountered with excessive turbine bearing clearances.

Whirl Mode Near Running Speed:

On the marine diesel engines, there are no speed controls on the turbochargers. This is a concern when the turbocharger is operated over 30,000 RPM. Figure 16 represents the eighth eigenvalue, which is the third forward critical speed. Note that this mode is at 33,000 RPM, which is 10% over design speed. There is a concern that if the turbocharger is over-sped, that this mode could be excited, leading to possible compressor rubs.

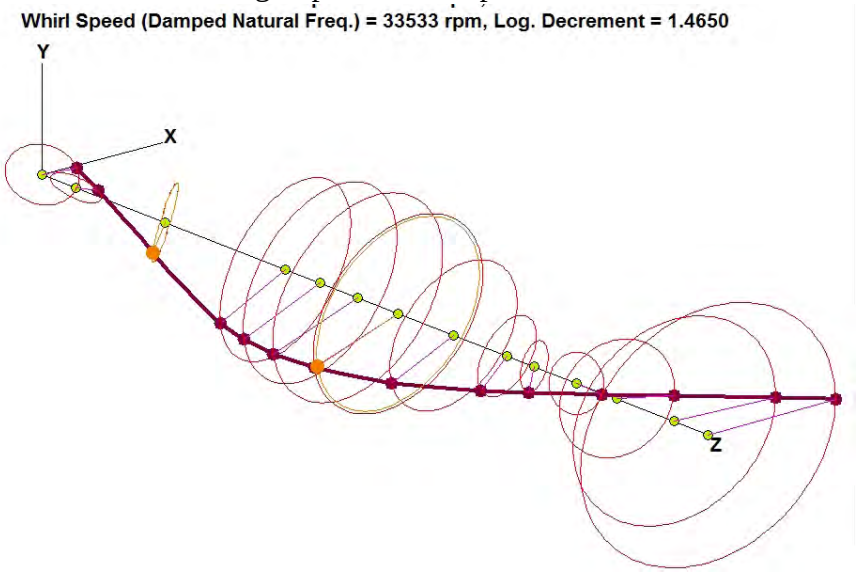

Fig 16. Turbocharger Bending Mode Above Running Speed at 33,500 RPM

In this mode, it is seen that the maximum amplitude occurs at the compressor location.

Locked Compressor Bearing Leading to Failure:

Under marginal lubrication conditions and tight compressor bearing inner clearances, the compressor bearing may weld onto the shaft. When this occurs, the floating bush bearing essentially becomes a plain bearing with a large clearance. The result of a locked bearing causes a very strong subsynchronous conical whirling to occur with large motion at the compressor. This frequency is predicted to be about 7,500 RPM. To compound the problem, the third forward critical speed drops down further into the operating speed range. Thus, the frozen, or locked, compressor bushing bearing leads to immediate turbocharger failure, usually resulting in shearing of the shaft under the compressor bearing as shown in Figure 17.

Figure 17 shows the effect of a rub on the compressor wheel. The blades are stripped, and the compressor has sheared the shaft under the compressor bearing. Once the inducer section or compressor wheel initiates a rub on the volute, the gyroscopic moments of the wheel reverse moment direction and tend to cause the wheel to precess backwards in the casing. This leads to rapid and extensive damage that is difficult to catch in time to avoid a total catastrophic compressor, inducer and shaft failure.

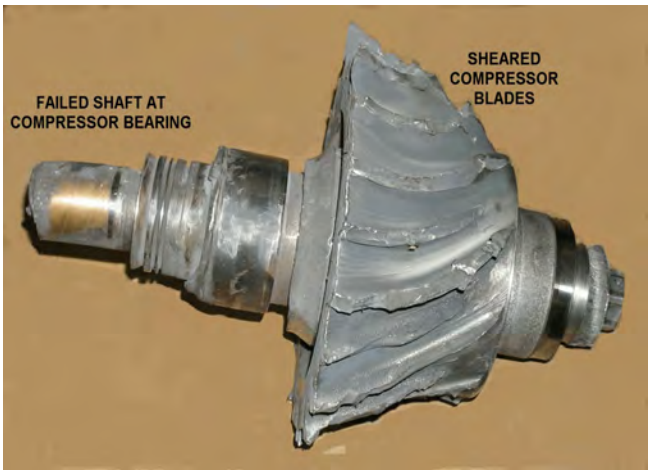

Fig.17 Failed Compressor and Shaft After Heavy Rub

When the floating ring seizes to the shaft, the bearing becomes a plain journal bearing. The stability characteristics of the plain journal bearing are quite poor and prone to self excited whirl instability at lower speeds dependant upon the bearing clearance. In fact a remarkable approximate equation to estimate the stability of a plain journal bearing is given as follows:

$$\omega s = 2.45\sqrt{\frac{g}{C}}, rad/Sec \tag{1}$$

For the case of the locked compressor ring bearing with a diametral clearance of 5 mils, the estimated stability threshold for the plain bearing, neglecting flexible shaft effects is predicted to be:

$$Ns = 2.45\sqrt{\frac{386}{.0025}} \times \frac{60}{2\pi} = 9,200 RPM \tag{2}$$

The above equation is an approximation of the threshold of stability for the plain journal bearing with a diametral clearance of 5 mils. This speed is less than one third of the operating speed of the turbocharger. Thus the floating ring compressor bearing welded

to the shaft may be expected to be highly unstable. To illustrate in more detail the stability characteristics with a locked compressor ring bearing, the actual bearing coefficients have been computed using the outer ring clearance and diameter as bearing parameters. Figure 18 represents the bearing coefficients generated at 30,000 RPM with the 5 mil clearance and 30 lb radial loading.

The bearing is operating at a low eccentricity ratio and very high attitude angle. This implies that the bearing stiffness cross coupling coefficients will greatly exceed the principal stiffness values.

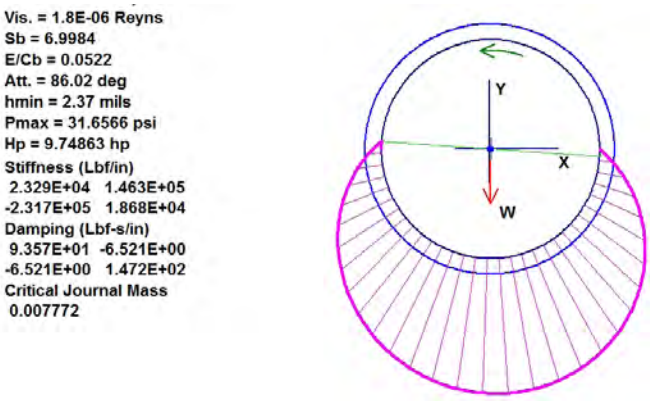

Fig. 18 Locked Compressor Bearing Characteristics at 30,000 RPM

For example, Figure 18 shows that the direct stiffness value Kxx is 23,300 Lb/In while the cross coupling coefficient Kyx is -232,000 Lb/In. This value is an order of magnitude higher than the direct stiffness values. This implies that the turbocharger operating at 30,000 RPM with a compressor ring bearing frozen to the shaft will be highly unstable.

In order to determine the degree of instability and the resulting turbocharger mode shape, a stability analysis was performed using the bearing coefficients as shown in Fig. 18. Figure 19 represents the first conical mode of the turbocharger with the seized compressor bearing. This highly unstable mode has a predicted whirl frequency of 7,500 CPM and a negative log decrement of -2.1.

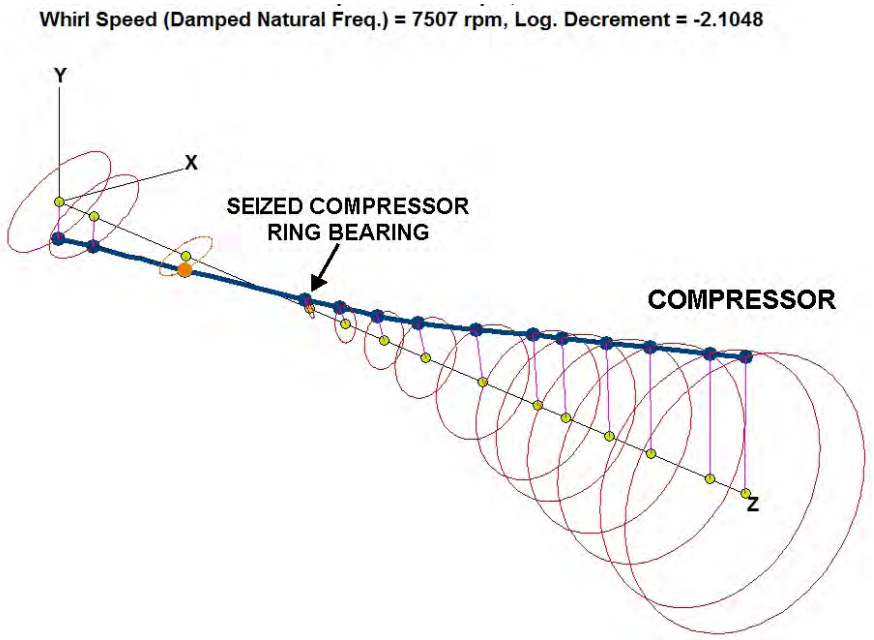

Fig. 19 Unstable Conical Whirl Mode at 7500 CPM With Seized Compressor Ring Bearing, Log Dec δ = -2.1

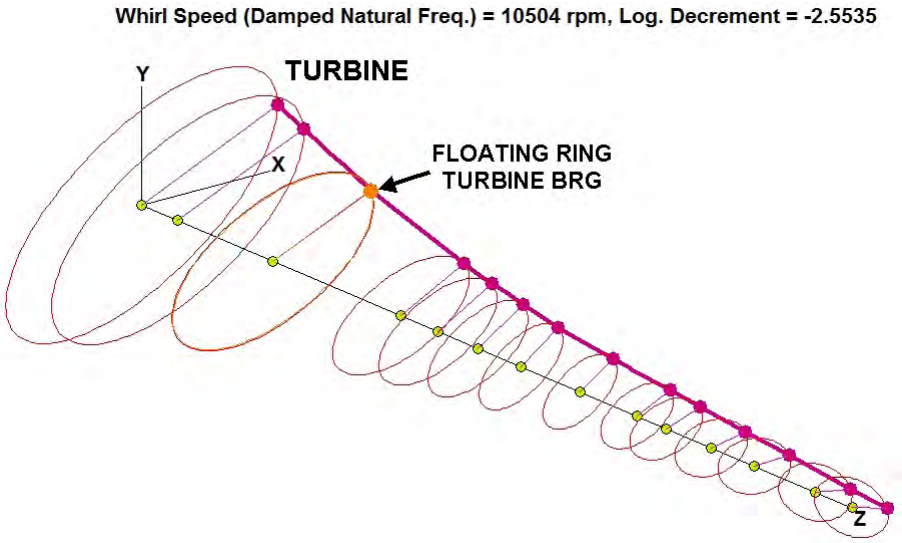

Fig. 20 Unstable Cylindrical Whirl Mode at 10500 CPM With Seized Compressor Ring Bearing, δ = -2.55

The seized compressor ring bearing also causes a second higher in-phase unstable cylindrical mode to occur. This mode has a high negative log decrement of -2.55 and a whirl frequency of 10,500 CPM. Thus it is possible for the turbocharger to exhibit two unstable modes. An FFT analysis of the rotor motion may show that both modes may be present. It is of interest to note that the simplified stability criterion for the plain bearing predicts the rigid body stability to be at 9,200 RPM. The finite element flexible rotor analysis predicts two unstable modes to occur with frequencies at 7,500 CPM and 10,500 CPM while operating at 30,000 RPM. In the past it appears that all recorded vibration data had been filtered to remove frequencies below 450 Hz. Therefore, subsynchronous vibrations on this class of turbochargers has not been properly documented or observed. Therefore failure can occur without adequate warning.

Nonlinear Time Transient Motion With Floating Ring Bearings:

In order to determine the dynamical motion of the turbocharger in the nonlinear floating bush bearings, a nonlinear time transient numerical analysis must be performed. Figure 21 represents the transient motion of the rotor for 50 cycles of shaft motion. The turbocharger is modeled by 14 major mass stations each with 4 degrees of freedom. The masses of the floating bush bearings represent another 4 degrees of freedom.

Thus for each time step, it is required to integrate 60 equations of motion and solve the finite element fluid film bearing equations for the forces generated on the inner and outer ring surfaces of the two floating bush bearings. In order to maintain accuracy of the orbits, 2000 time steps were used for each cycle of shaft motion.

The numerical computations were performed using the Runge-Kutta procedure as a starting solution. After several cycles of shaft motion, the solver is switched to the Newmark-Beta method which is faster but is not a self starter with zero initial conditions. In addition to the gravitational loads, an aerodynamic cross coupling force of 500 Lb/In is assumed to be acting at the compressor. Also in the model is a radial unbalance of 0.2 oz-in acting on the compressor wheel.

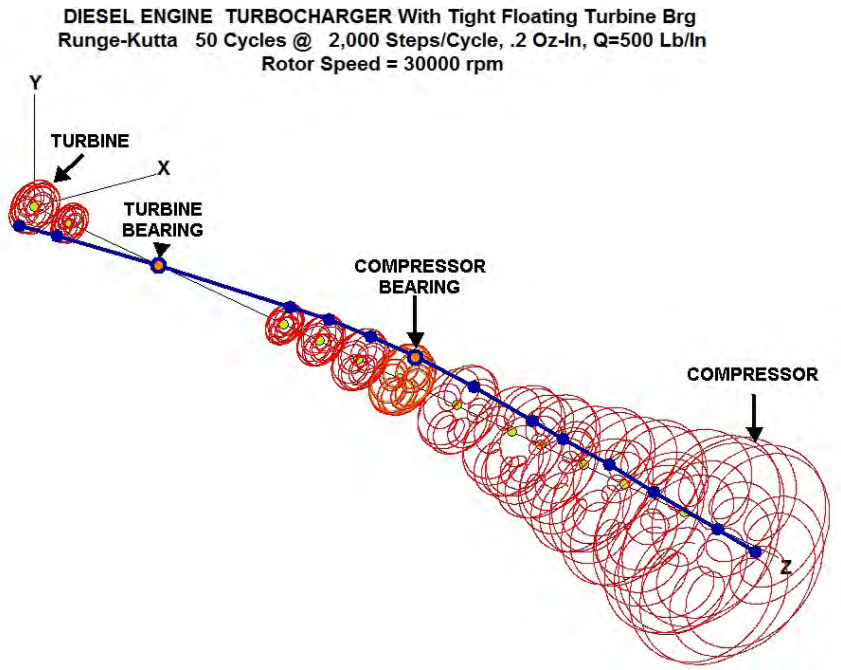

Fig. 21 Time Transient Motion of Turbocharger with Tight Turbine Brg, Q=500 Lb/In & 0.2 Oz-In Unbalance

Figure 21 represents the nonlinear turbocharger transient motion for 50 cycles of shaft motion. The orbital motion clearly shows subsynchronous whirling to be present in the system with the tight clearance floating ring turbine bearing and nominal clearance compressor ring bearing. For the case of assumed linearized bearing coefficients the transient whirl orbits would become unbounded. The orbital motion shown with the nonsynchronous whirl motion is bounded due to the nonlinear effects of the bearings. The nonsynchronous whirl motion greatly exceeds the synchronous response caused by the unbalance of 0.2 oz-in acting at the compressor wheel.

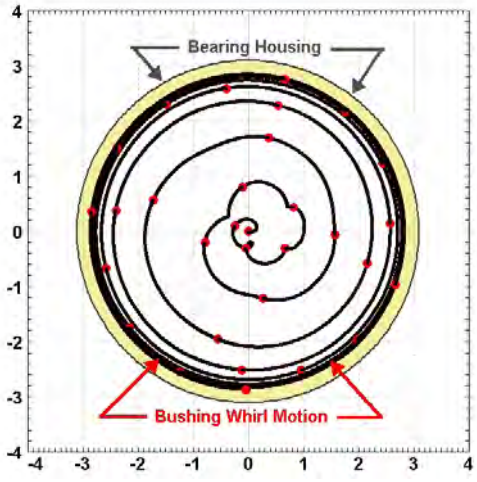

Fig. 22 Bushing Motion, Mils

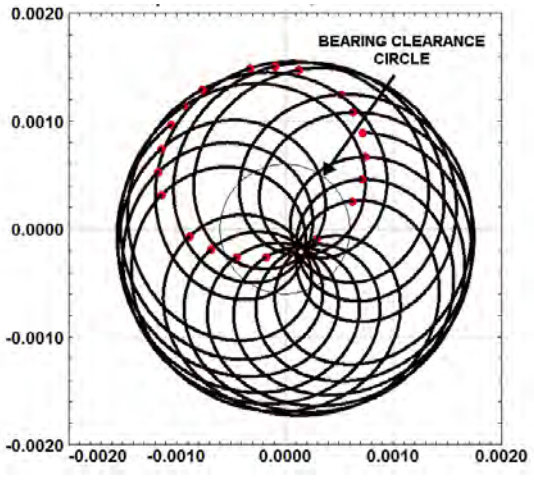

Fig. 23 Motion At Compressor Brg *(Inches)*

Figure 22 represents the motion of the compressor bushing in the housing. Notice that the whirl orbit fills up over 80 % of the bearing clearance.

On Figure 22 are placed timing marks to represent each shaft revolution. The motion initially starts off with a small component of synchronous precession and then becomes dominated by the subsynchronous whirl motion. The scale on Figure 22 is in mils. The compressor bushing is orbiting with over 5 mils of motion. This large motion will cause much higher bearing forces to be transmitted than if one had only synchronous precession caused by the 0.2 oz-in of unbalance. The specified unbalance of 0.2 oz-in causes a rotating load of about 320 lb at 30,000 RPM. This level of unbalance is equivalent to the mass center of the compressor to be displaced from the axis of rotation by approximately 1 mil.

Figure 23 is the absolute motion of the shaft at the compressor bearing location. The resulting bounded limit cycle orbit is a combination of synchronous precession due to unbalance and the lower frequency subsynchronous whirl motion. Note the size of the compressor inner ring clearance as compared to the total orbit observed at the compressor bearing.

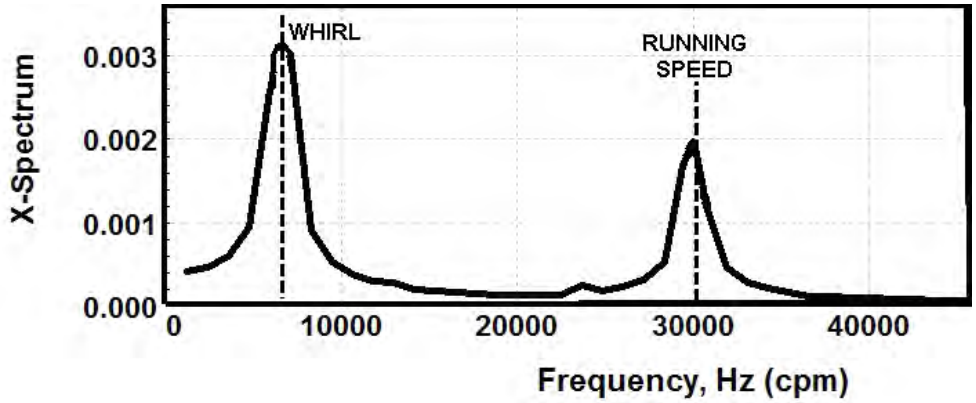

Fig. 24 FFT of Absolute Compressor Bearing Motion Showing Subsynchronous Whirling

Figure 24 represents the FFT analysis of the motion of the compressor bearing station as shown in Figure 16. It is seen that the motion is composed of synchronous precession caused by the rotor unbalance and the lower self-excited whirl motion that is inherent with the floating bush bearings. If one filters the frequency data below 500 Hz, as is common practice, then it is apparent that the important whirling motion will not be observed! It is seen that the whirl motion is 3 mils of amplitude as compared to the 2 mils of synchronous motion created by the rotating unbalance load. One may surmise that if the bearing were perfectly stable, then the total amplitude of motion should be reduced by 3 mils. Figure 25 represents the motion of the compressor inducer. Drawn on this figure is the inducer clearance circle of the stator vanes. Rubbing will occur when this orbit exceeds the operating clearance causing blade contact.

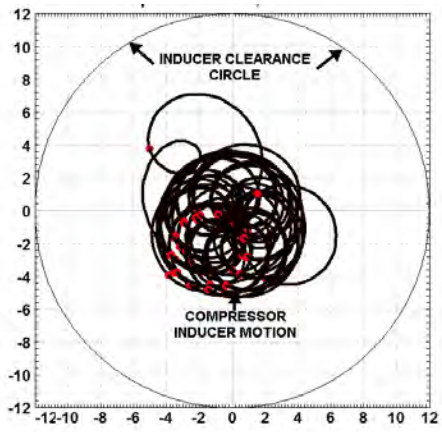

Fig. 25 Inducer Motion, Mils

Compressor Floating Ring Bearing Forces Transmitted:

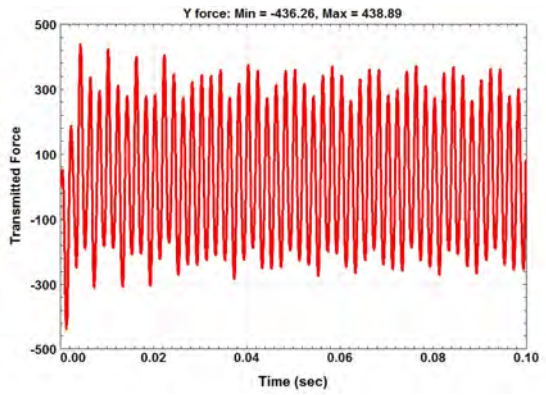

Fig. 26 Compressor Brg Forces With 0.2 Oz-In Unbalance

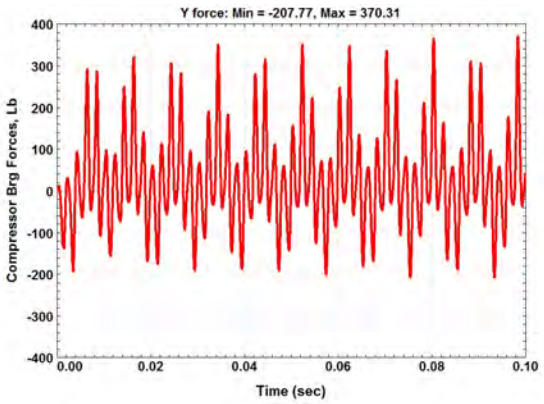

Fig. 27 Compressor Bearing Forces With Balanced Rotor

Figure 26 shows the large bearing forces of over +-430 Lb with the 0.2 oz-in of unbalance. These large transmitted compressor bearing forces are not due to unbalance alone. Figure 27 shows the compressor floating ring bearing forces for a balanced rotor. With a perfectly stable rotor system, there should be no dynamic loads after the initial transient vibration dies out after the first few cycles of shaft motion.

Figure 27 shows dynamic loads being transmitted with forces as high as 370 Lb. This transmitted loading for the case of a balanced rotor represents a loading which exceeds the bearing static loading by over a factor of 10. These high dynamic forces are generated by the large amplitude whirling motion that is inherent in all floating ring bearings. It is apparent that in order to achieve limit cycle motion, that high bearing forces must be generated. These high bearing loads may eventually lead to overheating of the bearing and tar and varnish formation on the inner surface of the compressor floating ring bearing. Such operating conditions lead to reduced bearing life.

Motion with Large Clearance Turbine and Compressor Bearings:

There is a range of allowable clearances specified for both the compressor and turbine floating bush bearings. The maximum specified values for the floating bush turbine bearing is approximately 3 mils for the inner clearance and 10 mils for the outer clearance.

Figure 28 represents the nonlinear transient motion for 50 cycles of shaft motion with larger clearances on the turbine floating ring bearing. The larger turbine ring clearances leads to a pronounced conical whirling motion with high amplitudes at the compressor and inducer sections.

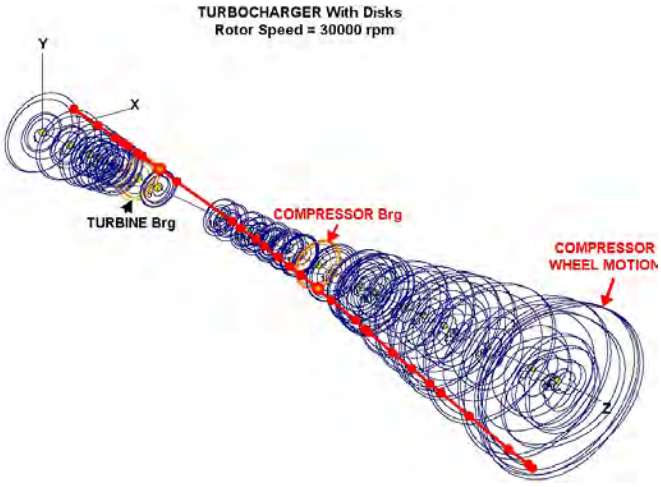

Fig. 28 Transient Motion With Large Clearance Turbine Bearing

Figure 29 represents the turbine bushing motion with the large inner and outer bushing clearances. The initial transient motion starts out in a controlled limit cycle motion influenced by the rotating unbalance forces acting on the compressor wheel. The motion then changes into a large limit cycle motion with a conical motion as shown in Figure 28.

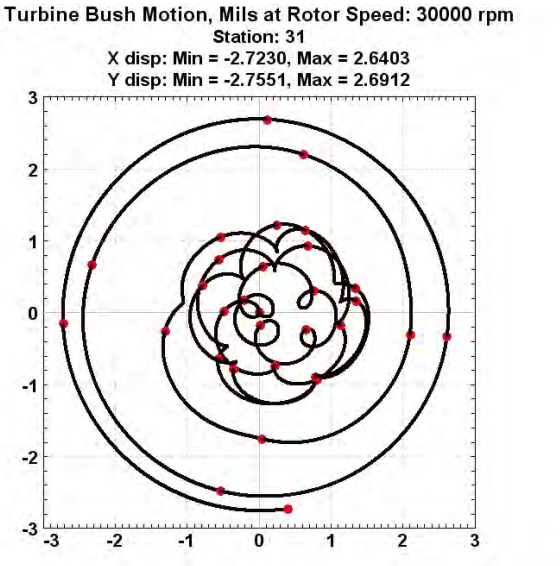

Fig. 29 Turbine Bushing Motion With Large Clearances, Mils

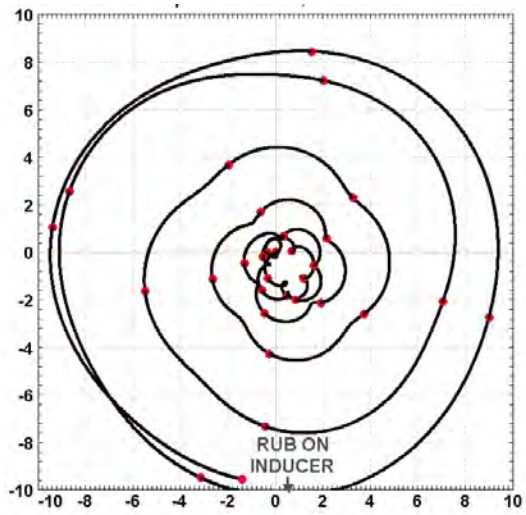

Fig. 30 Excessive Inducer Motion Caused By Large Turbine Brg Cl

Figure 30 shows the resulting motion at the compressor inducer section. This large motion will lead to rubbing on the inducer section of the compressor wheel which will initiate failure.

Figure 31 represents the compressor bearing forces transmitted with the large prescribed turbine bearing clearances. The initial transient motion starts out with a small controlled limit cycle motion caused by the applied unbalance at the compressor wheel. After about 22 cycles of shaft motion, the motion of the system jumps into a large conical whirling mode with a rapid increase in the bearing forces transmitted. Compressor bearing forces increase to over 400 lb.

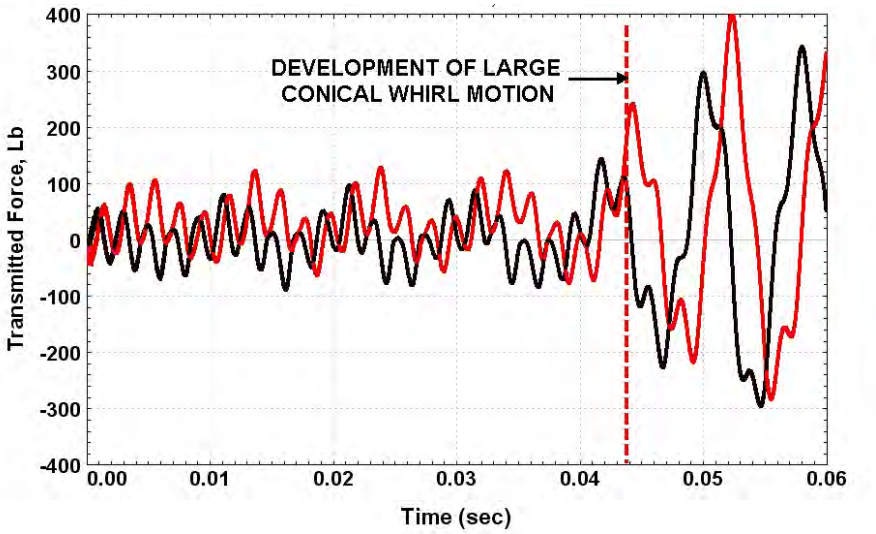

Fig. 31 Compressor Bearing Forces Transmitted With Large Clearance Floating Bush Turbine Bearing

Figure 32 represents the turbocharger motion with nominal turbine clearances of 2 mils for the inner ring and 6 mils for the outer ring. The compressor bearing has increased ring clearances from 1 to 2 mils on the inner ring and from 5 to 10 mils for the outer ring clearance. Added to the dynamical analysis is 0.2 oz-in of unbalance on the compressor wheel. The circle shown on the figure represents the clearance margin between the inducer section of the compressor and the stationary stator vanes.

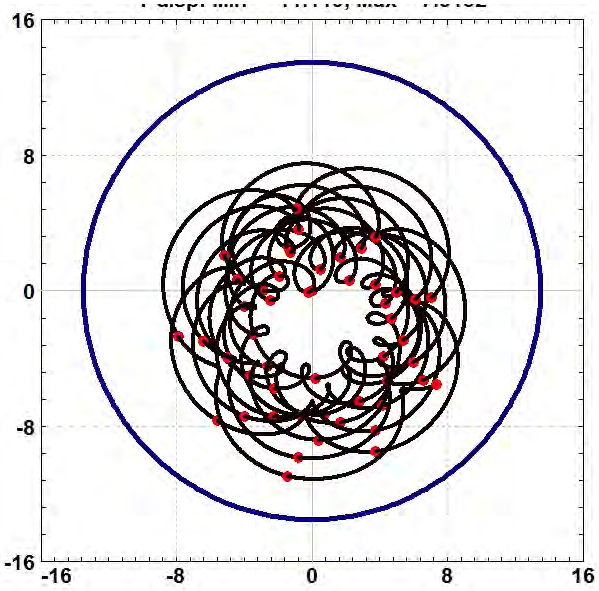

Fig. 32 Motion at Inducer With Large Compressor Ring Bearing Clearances

Note that the orbital path is offset from the clearance circle. This is due to the gravitational loading on the compressor. The motion is clearly in subsynchronous whirling. The repeated internal loops are caused by the rotating unbalance load. The motion is clearly in a well defined limit cycle whirl which is not in contact with the stator. It is apparent that the size of the limit cycle motion at the compressor and inducer location is strongly influenced by the turbine ring bearing clearances. The turbine ring clearances must be closely controlled in order not to have excessively large compressor-inducer whirling.

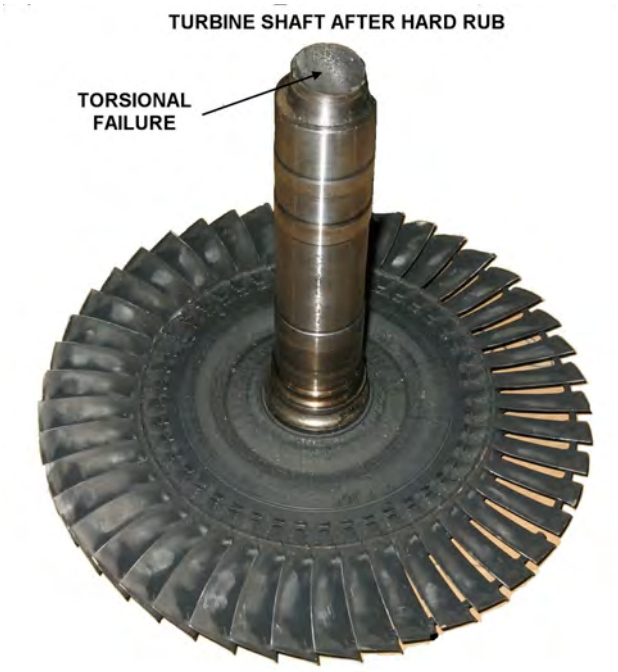

Figure 33 Steel Turbine Shaft After Hard Compressor - Inducer Rub

Figure 33 represents the welded steel shaft and turbine assembly after a hard rub. Examination the shaft failure indicates a torsional failure. This failure occurs under the compressor bearing.

Stability With Axial Groove Floating Bush Bearings:

Figure 34 represents a floating bush bearing in which 3 axial grooves have been added to the inner ring of the bearing and 4 grooves have been placed into the stationary bearing housing. This creates a 4 axial groove bearing for the outer ring.

The concept for the use of the axial grooves is two-fold. The first objective is to improve the lubricant supply to the inner and outer bearing surfaces. The second objective is an apparent attempt to improve the stability characteristics over a plain journal bearing.

The apparent attempt to promote stability and improved lubrication of the floating ring bearings by the use of axial grooves is not effective.

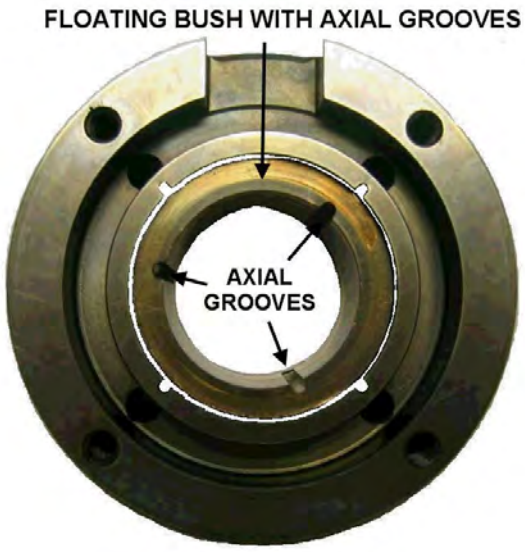

Fig. 34 Floating Bush Bearing With Axial Grooves

TC Compressor Brg- Min Cl-40000
L= 0.945 in, D= 1.3185 in, Cb= 0.0004 in, 2Cb/D=0.000607, m= 0, tilt= 0.5
Speed = 40000 rpm
Load = 30 Lbf
W/LD = 24.0774 psi
Vis. = 1E-06 Reyns
Sb = 75.211
E/Cb = 0.0048
Att. = 88.80 deg
hmin = 0.3981 mils
Pmax = 59.2691 psi
Hp = 10.3533 hp
Stiffness (Lbf/in)
1.178E+05 3.946E+06
-1.562E+07 1.072E+05
Damping (Lbf-s/in)
1.884E+03 -4.009E+01
-4.009E+01 7.458E+03
Critical Journal Mass
0.01495

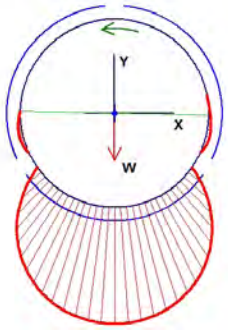

Fig. 35 3 Axial Groove Inner Bearing Zero Preload, Cd = 0.8 Mils

Vis. = 1.8E-06 Reyns
Sb = 2.2533
E/Cb = 0.2805
Att. = 75.69 deg
hmin = 1.799 mils
Pmax = 52.9428 psi
Hp = 0.491808 hp
Stiffness (Lbf/in)
1.442E+04 2.419E+04
-4.819E+04 2.802E+04
Damping (Lbf-s/in)
5.140E+01 -1.312E+01
-1.312E+01 8.771E+01
Critical Journal Mass
0.0656

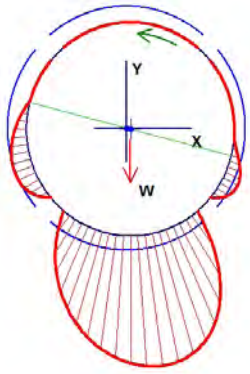

Fig. 36 4 Axial Groove Outer Bush Bearing

Figure 35 represents the pressure distribution for the inner ring with 3 axial grooves. Figure 35 shows the pressure distribution and stiffness and damping coefficients for the compressor bearing as shown in Figure 34 for a static loading of 30 lb and minimum specified diametral of .8 mils. Note that with the load vector directed towards the bottom arc, the other two arcs have not generated a pressure profile. The corresponding bearing coefficients are shown in Table 4 for the inner ring. These bearing coefficients are reduced as compared to the coefficients as shown in Table 2.

Figure 36 represents the outer ring bearing which has 4 axial grooves in the stationary housing. The coefficients for the outer ring are shown in Table 4. These bearing values are reduced from those presented in Table 2. It is thus concluded that the use of axial grooves reduces the bearing stiffness and damping values for both the inner and outer rings. Similar conclusions may also be obtained for the turbine end floating bush bearing.

Table 4 Axial Groove Compressor Bush Bearing Coefficients - 30,000 RPM *(Lb/In)*								
	K_{yy}	K_{xy}	K_{xx}	K_{yy}	C_{xy}	C_{xx}	C_{xx}	C_{yy}
Inner	**.118E6**	**3.95E6**	**-15.6E6**	**.107E6**	**1884**	**-40**	**-40**	**7460**
Outer	**14,420**	**24,200**	**-48,200**	**28,600**	**51**	**-13**	**-13**	**88**

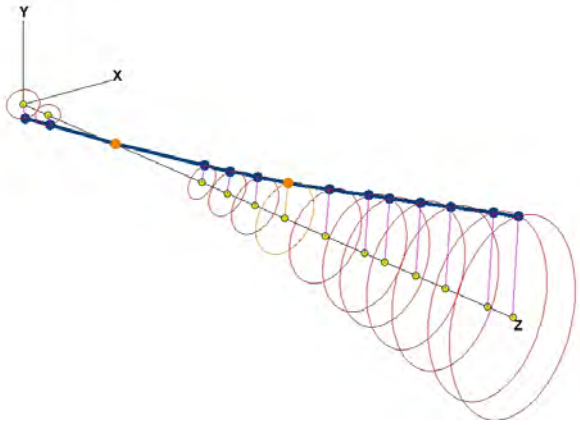

Fig. 37 Unstable 1st Forward Mode
Nf1 = 4902 CPM, ζ = -0.135

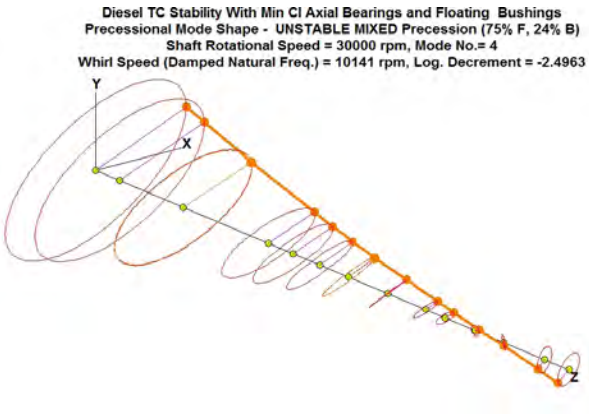

Fig. 38 Unstable 2nd Forward Mode
Nf2 = 10,141 CPM, ζ = -2.5

A stability analysis was performed on the turbocharger based on the bearing coefficients of Table 4 for the floating ring bearings with axial grooves. Figure 37 represents the first forward mode which is a conical mode with an unstable log decrement of -0.135 and a whirl frequency of 4,900 CPM. Note that the softer bearing coefficients has reduced the whirl of the first mode. As expected, this first conical mode is basically controlled by the characteristics of the compressor bearing.

Figure 38 represents the second forward mode at a whirl frequency of around 10,100 CPM. This mode has a large negative log decrement 0f -2.5. It is possible for both of these modes to be excited and present in the vibration spectrum.

Figure 39 represents the third system forward mode at 30,325 RPM. Thus the use of axial groves in the floating bush bearings cause such soft bearing coefficients that the third forward mode is lowered into the operating speed range.

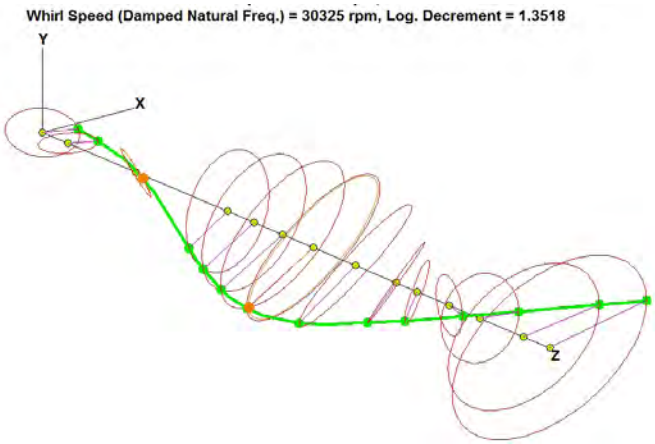

Fig. 39 3rd Mode at Speed, Nf3 = 30,325 RPM

Turbocharger Dynamics With Three-Lobed Compressor Bearing:

The floating bush compressor bearing is not an ideal design for the large diesel engine turbochargers. This type of bearing is always inherently unstable. It is seen that in order to have controlled limit cycle motion, the inner clearances in the compressor and turbine ring bearings must be kept very tight. This is particularly true for the compressor inner ring clearance. The required tight clearance may lead to over heating and seizure of the compressor ring to the shaft. A more suitable design is the use of a three-lobed bearing. Figure 40 represents the pressure profile of a three-lobed bearing with a 90% converging film thickness and a preload factor of m = 0.5. The 3 axial groove bearing would be represented by a preload of m=0. Without preload, no pressure is generated for the case of a centered shaft.

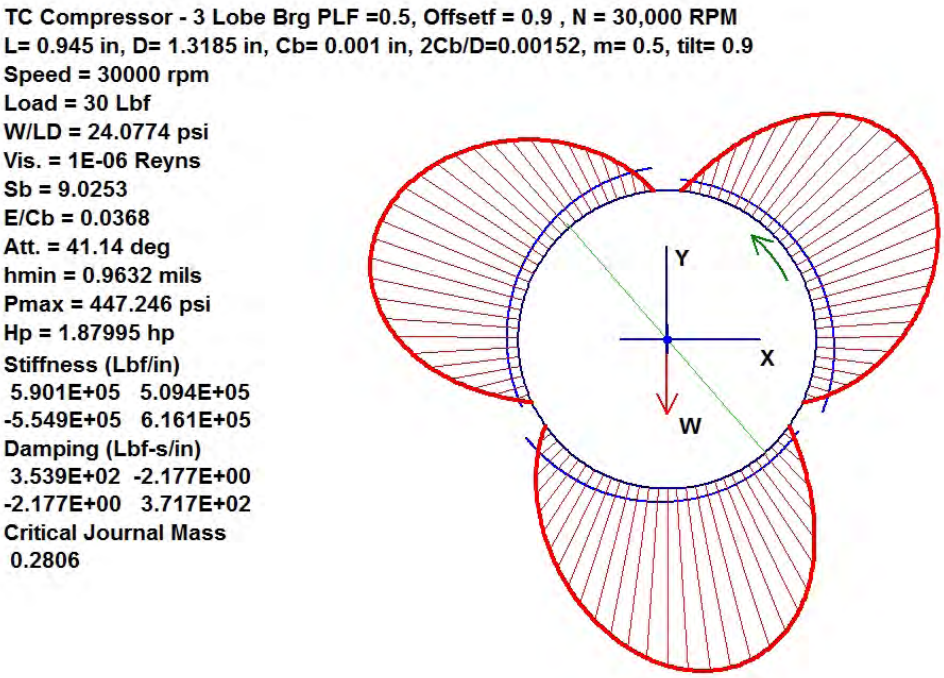

Fig. 40 3 Lobed Compressor Bearing Pressure Profile and Brg Stiffness and Damping Coefficients, m=0.5, Cd = 2 Mils

Each lobe is developing a positive pressure profile even when the shaft is centered. Thus 3 positive load vectors are generated by the bearing to help stabilize the shaft. The radial stiffness of this bearing has been greatly increased along with the damping, and also there is a reduction in the bearing cross-coupling coefficients. Since each sector of the bearing forms an active converging wedge, the radial clearance may be made larger then what is permissible with the axial groove bearing. This allows the bearing to run cooler.

The relative stability of any particular bearing design may be evaluated by the value of the bearing computed critical mass. The critical mass for the 3 lobed bearing as shown in Fig. 40 is 0.2806. This value multiplied by gravity of 386 in/sec^2 gives a value of 108. This implies that a rigid rotor that weights up to 108 lb will be stable at 30,000 RPM. This is in contrast to the computed value of only 0.015 for the axial groove bearing. This implies that a rotor with as little weight as 6 lb will be unstable at this speed.

The actual stability of the entire system must be computed by a complex eigenvalue analysis which includes the second bearing, shaft flexibility, and added aerodynamic cross coupling.

Figure 41 represents the turbocharger nonlinear transient motion at the inducer location with a rigidly mounted three-lobed compressor end bearing. Shown also on Figure 41 is the clearance circle of the inducer. The maximum motion at the tip of the compressor assembly is approximately ± 4.5 mils. This orbital motion is well within the inducer clearance circle so that no rubbing should. The whirl is in a well controlled limit cycle orbit. Since the synchronous timing marks on the orbit are not aligned, there is apparently some nonsynchronous precession in the motion.

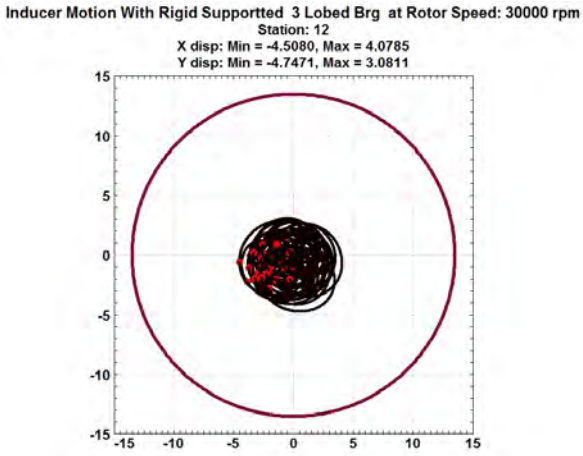

Fig. 41 Motion at Inducer With 3 Lobed Bearing on Rigid Supports

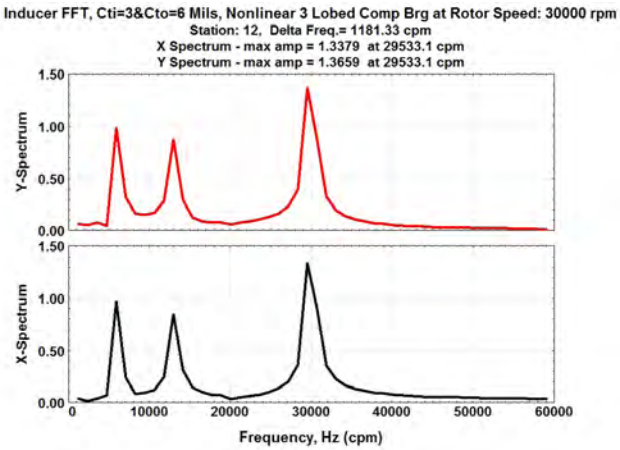

Fig. 42 FFT Analysis of Motion at Inducer

An FFT analysis of the compressor motion was performed as shown in Figure 42. There is present small components of both the conical and cylindrical whirl motions which are well controlled. The reason for the small amounts of whirl is that the turbine bearing has not been replaced by a three-lobed bearing design. As long as the turbine floating bush bearing clearances are kept tight, the turbocharger motion is well controlled with the three-lobed bearing compressor bearing.

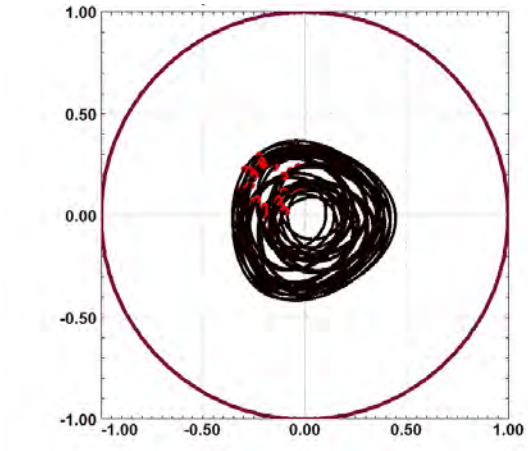

Fig. 43 Compressor Bearing Motion in 3 Lobed Bearing at 30,000 RPM

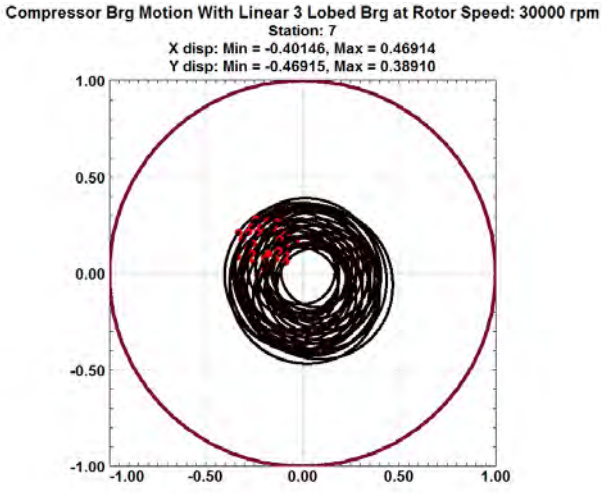

Fig. 44 Bearing Motion With Linear Coef.

Figure 43 represents the motion at the compressor bearing with the nonlinear 3 lobed bearing. Note that the orbit has a three lobed shape due to the bearing design. In order to compute the motion, the 3 lobed bearing forces must be computed at each time step.

If, instead of computing the pressure profile and bearing lobe forces at each time step, the linearized bearing coefficients, as shown in Figure 40 may be used instead. The resulting bearing orbit is shown in Figure 44. The computational time required using the linearized three lobed compressor bearing stiffness and damping coefficients is over 100 times faster than the nonlinear analysis. It is remarkable, that in this case, the resulting linearized analysis is less than 10% in error both in amplitudes and bearing forces transmitted. This implies that the bearing stiffness and damping coefficients may be used for a very accurate stability analysis.

Figure 45 represents the time transient motion of the turbocharger with the fixed 3 lobed compressor bearing and the floating bush turbine bearing. Due to the high stiffness of the 3 lobed compressor bearing, the motion at this location is quite small as compared to the motion at the floating bush turbine bearing location.

It is apparent from the examination of the orbital behavior for 25 cycles of motion that the source of the observed subsynchronous whirl components as shown by the FFT analysis is the result of the floating bush turbine bearing. Therefore, to achieve maximum stability, the floating bush turbine bearing needs to be also replaced by a 3 lobed bearing configuration.

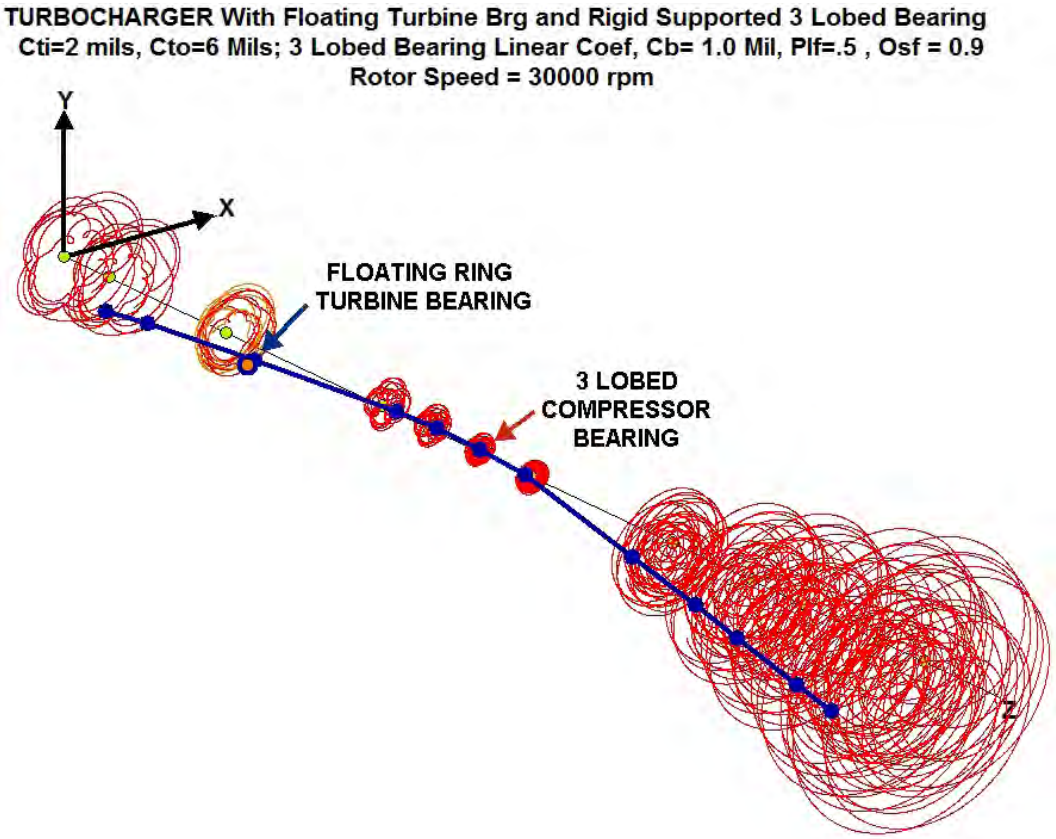

Fig. 45 Time Transient Turbocharger Motion With Fixed 3 Lobed Bearing and Floating Bush Turbine Bearing

In the analysis of the compressor bearing forces transmitted, it was observed that these forces have been significantly reduced over the bearing forces transmitted for the case of the floating ring compressor bearing. This is due to the smaller orbits at the bearing location. Large whirl motion leads to high bearing forces transmitted and elevated bearing temperatures. It is also apparent that accelerometers placed at the compressor and turbine locations would record considerably different magnitudes and frequencies of motion.

Turbocharger Dynamics With Three-Lobed and Squeeze Film Damper Bearings:

The turbocharger will be stable with two rigidly mounted three lobed bearings. However there is an advantage to having the bearings loosely mounted with outer bearing clearance values similar to those used in the floating ring bearings. If, in addition, the bearings are pinned to prevent rotation, then in essence, we have unconstrained squeeze film dampers acting in series with the three lobed turbine and compressor bearings.

For the land based diesel engine turbochargers, the fixed lobe design should be adequate. However, for marine based diesel engine turbochargers, the incorporation of the squeeze film dampers has several distinct advantages. Various smaller vessels operated by the Navy and Coast Guard, for example, operate at high speeds and in heavy seas. These conditions generated manouevre loads on the compressor and turbine wheels. The use of squeeze film dampers help protect the turbocharger from high transient loads and impacts during operation. Such transient loads would not be experienced by the typical locomotive turbocharger operating under constant speed conditions.

The precession of the bearing ring generates both a radial stiffness and damping values which are nonlinear with respect to eccentricity and speed of rotation. For the assumption of circular synchronous precession about the damper origin, the radial damper stiffness is:

$$K_D = \frac{2\mu R \varepsilon \omega}{\left(1-\varepsilon^2\right)^2}\left(\frac{L}{C}\right)^3 \tag{3}$$

The damping is given by:

$$C_D = \frac{\mu R \pi}{2\left(1-\varepsilon^2\right)^{3/2}}\left(\frac{L}{C}\right)^3 \tag{4}$$

The radial stiffness value for the squeeze film damper is a highly nonlinear function of the damper eccentricity ratio varying from 0 in the centered position to a theoretical value of infinite for eccentricities approaching unity. This condition is referred to as damper lockup. In general, we do not wish to have dampers operating with eccentricity values greater than 0.5.

The squeeze film damping value is fairly uniform for eccentricities up to 0.4. Its value is a much more uniform change with eccentricity. Note that in both cases, the damping and stiffness vary as the cube of the L to C ratio. Therefore, small changes in clearance can have a dramatic effect on the damper properties.

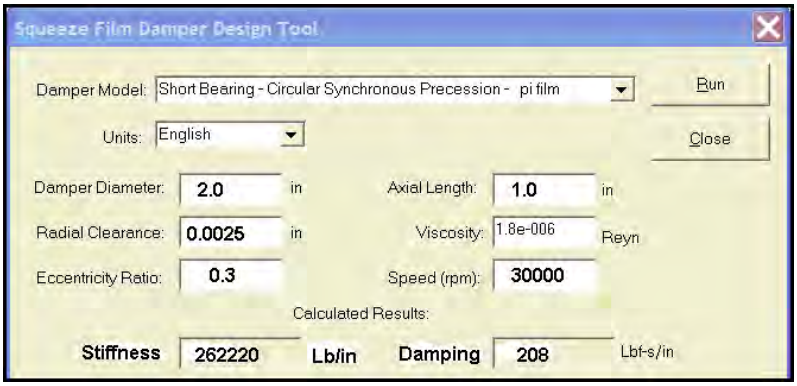

Table 5 Squeeze Film Stiffness and Damping
L = 1 in, Cr = 0.0025 in, ec = 0.3, N = 30,000

Table 5 represents a Dyrobes tool for computing the synchronous stiffness and damping for a squeeze film damper for an assumed eccentricity ratio and speed for a given damper design. In this case the damper length is 1 inch and the radial clearance is 2.5 mils (0.0025 in.). With the assumed orbital eccentricity, the radial computed stiffness is approximately 260,000 lb/in and the damping is 208 lb-sec/in. These values will be used in a stability analysis of the turbocharger assuming 3 lobe bearings incorporated with the dampers. These bearings would require no more space than what was required with the original floating bush bearings. The main difference is that the 3 lobed bearings are pinned to prevent rotation.

Figure 46 represents mode 5 of a damped eigenvalue analysis with the 3 lobed bearings mounted in squeeze film damper bearings as shown in Table 5. Included in the stability analysis is the destabilizing cross coupling coefficient of 500 lb/in acting at the compressor. The 5th mode is actually the first forward conical mode. The lower modes are either backward or critically damped.

With the positive log decrement of 0.65, this mode is highly stable. Note that the amplitudes of the turbine bearing and damper are very small in comparison to the motion at the compressor bearing location. Hence the use of linearized bearing coefficients for the turbine bearing is very accurate as the turbine bearing strain energy is small. This conical mode is controlled by the characteristics of the compressor bearing. Note that the more effective 3 lobed bearing and damper configuration has raised the first conical mode from around 4,900 RPM to over 10,000 RPM. The log decrement represents a critical speed amplification factor of 3.14/0.652 = 4.8. Thus the turbocharger should be well behaved when passing through the first critical speed which has now been raised to over 10,000 RPM.

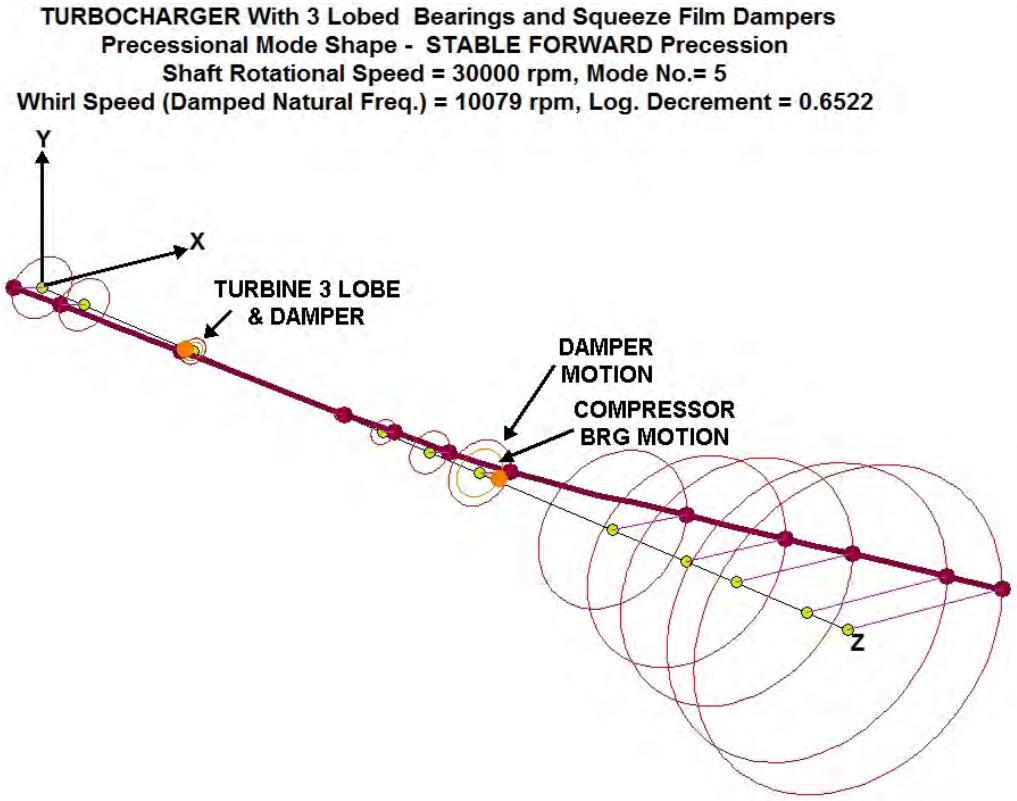

Fig. 46 Stable 1st Conical Mode With 3 Lobed Bearings Mounted in Squeeze Film Dampers

In order to further understand the stability of the turbocharger in the 3 lobed bearings, a time transient analysis was performed which includes the full nonlinear compressor damper bearing along with the influence of gravity, aerodynamic cross coupling and compressor unbalance. Figure 47 shows the transient motion for 25 cycles of motion. After the first several cycles of motion, the shaft orbits are all synchronous precession. There is no subsynchronous whirling in the system. The system is totally whirl free.

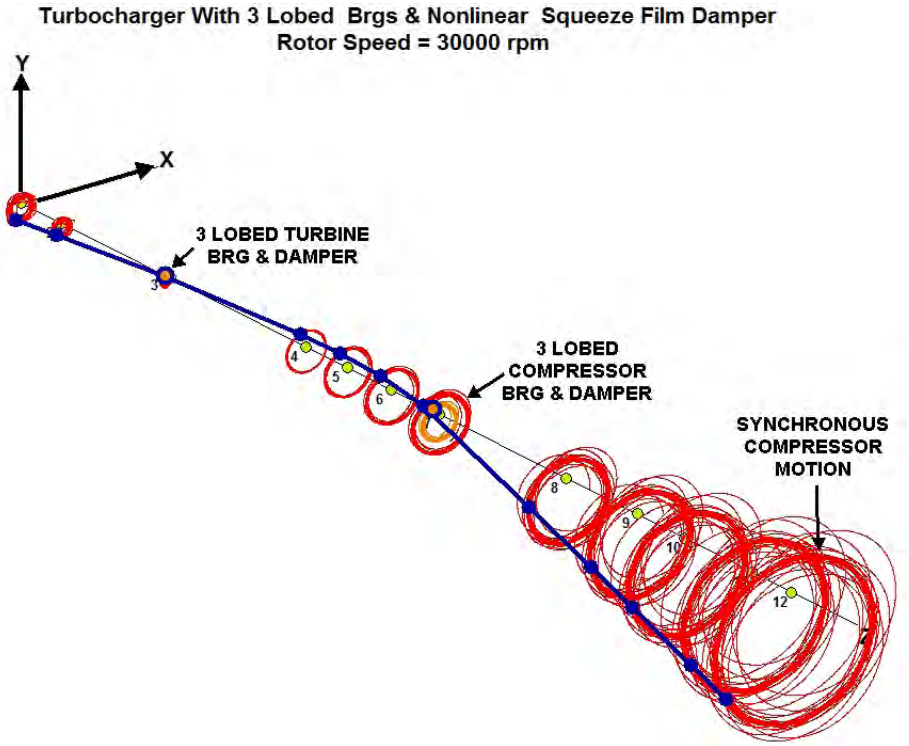

Fig. 47 Transient Motion With 3 Lobed Brgs & Nonlinear Compressor Damper, Unbalance = 0.2 Oz-In, Qaero =500 Lb/In

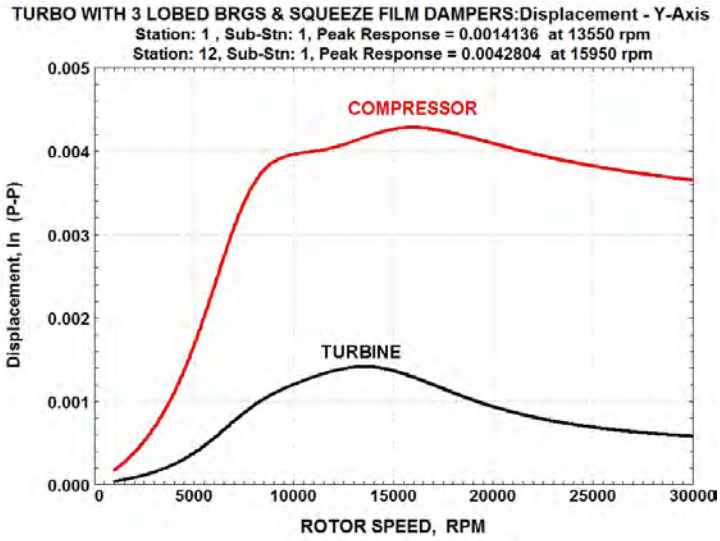

Fig.48 Unbalance Response With Nonlinear Compressor Damper, Ub=0.2 Oz-In

Figure 48 represents the forced unbalance response of the turbocharger with the combination of the 3 lobed bearings in nonlinear squeeze film dampers. The motion is well controlled.

Discussion and Conclusions:

The reliability of large diesel engine turbochargers using floating bush bearings may be greatly improved by the replacement of these bearings by the three lobed bearing design mounted in squeeze film dampers. Since the three lobed bearing is more effective in generating a positive pressure profile, a larger bearing clearance may be employed which leads to a cooler operating compressor bearing. The use of axial grooves in the floating bush does not improve stability, but actually leads to larger whirl orbits.

For the case of the floating bush bearing design, it is seen that both compressor and turbine bearings must have close clearances in order to achieve a controlled limit cycle of motion to prevent compressor rubbing. Even for the case of the improved three lobed bearing design, this may not prove to be sufficient if the lubricant and filtration system is not improved. The turbochargers are normally lubricated with the same oil used in the diesel engine. The operating conditions in diesel engines are much more severe than in automotive engines. As a general rule in all high-speed turbochargers, whether diesel or automotive, should employ of a high-quality PAO (polyalphaolefin). Conventional lubricants do not meet the requirements necessary for the adequate and reliable performance of high-speed turbochargers with respect to viscosity index, film strength, and coking temperature.

Figure 49 shows the wear comparison between a PAO lubricant with extreme pressure additives and a standard ISO 32 lubricant. This type of lubricant is highly recommended for all turbochargers because of the elevated temperature and loading conditions.

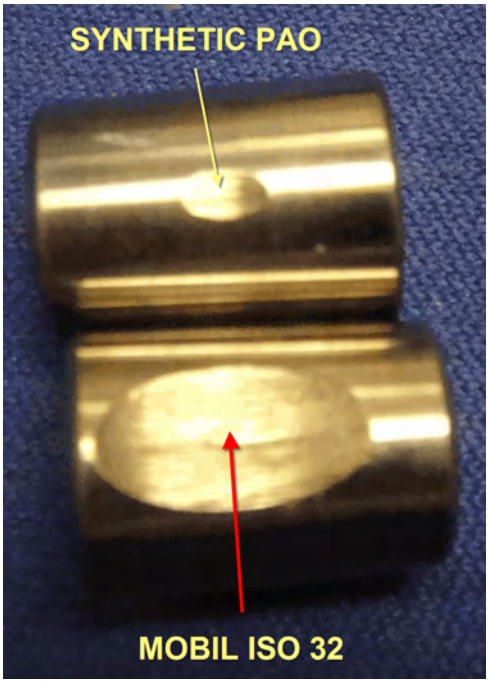

Fig. 49 Wear Comparison Between PAO & ISO 32 Lubricant

In addition to the use of a high quality PAO for these large diesel engines, it is also recommended that a secondary oil filter should be used for each turbocharger. Due to the more extreme operating conditions of a diesel engine, as compared to an automotive engine, it is imperative that any particle debris or carbon deposits be filtered before entering into the lubrication system of the turbocharger. Carbon particle buildup in the turbocharger may result in limited oil flow to the compressor bearing or enhance the condition of varnishing of the bearing surfaces. It is imperative to have a clean oil supply to the turbocharger bearings.

A more serious operating situation occurs with the marine diesel engines. These engines operate without speed control on the turbocharger. Therefore the turbocharger may exceed its design speed of 30,000 RPM. It is seen that with the axial groove floating bush design, the third critical speed may now possibly be excited by over speeding.

Another serious dynamic loading that occurs with marine engines is the action of the ship over high sea waves. The pitching motion of the vessel causes a change of the gyroscopic moment. This creates additional loads, referred to as maneuver loads, to act on the compressor and wheels. These effects are quite common with high-speed aircraft engines in fighter planes.

These additional moment loads, particularly on the compressor wheel, in addition to the higher operating speeds, can also induce rubs on the compressor wheel. This particular design of turbocharger is particularly susceptible to rubs, as it has a backward whirl mode near running speed. The backward mode causes the compressor to be locked against the volute causing it to whirl backwards. This leads to impeller damage or shaft failure.

To produce an increased safety margin of operation, the impeller inducer section and compressor wheel should have approximately 5 mils of material removed to increase the running speed clearances when operating with floating bush bearings. The application of the three lobed damper design will greatly improve reliability with this class of turbocharger as it will substantially reduce the orbital motion at the inducer section under all operating conditions..

While the cost of this type of bearing may not be warranted for automotive turbochargers, it is justified for this class of turbocharger with its much higher initial cost and improvement in reliability.

It is of interest to note that very little reliable experimental data has been obtained on these turbochargers. Most of the data is usually taken corresponding to running speed with the lower frequencies filtered out. However, it is the lower frequencies which represent the subsynchronous precession of the turbocharger which are of importance. It is recommended that vibration monitoring of the turbochargers be conducted to determine the magnitude and frequencies of the subsynchronous whirl motion.

BIBLIOGRAPHY

1. Chen, W. J., and E. J. Gunter, *Introduction to Dynamics of Rotor-Bearing Systems*, Trafford Publishing, Victoria, BC, Canada, (2007).
2. Barrett, L. E., and E. J. Gunter, "Steady State and Transient Analysis of a Squeeze Film Damper Bearing for Rotor Stability", NASA CR-2548, (1975)
3. Gunter, E. J., "Design of Nonlinear Squeeze Film Dampers For Aircraft Engines", ASME J. of Lubrication, vol. 92, No. 1, pp. 57-64, (1977)
4. Gunter, E. J., and W. J. Chen, "Dynamic Analysis of a Turbocharger in Floating Bush Bearings," ISCORMA-3, Cleveland, OH, (2005).
5. Kirk, R. G., A. Alsaeed, and E. J. Gunter, "Stability Analysis of a High-Speed Automotive Turbocharger," Proceedings of ASTLE/ASME International Joint Tribology Conference, San Antonio, TX, (2006).
6. Faulkenhagen, G. L., E. J. Gunter, and F. T. Schuller, "Stability and Transient Motion of a Three-Lobed Bearing System," ASME No. 71, Vib. 76, (1971).
7. Shaw, C. M., and F. Max, *Analysis and Lubrication of Bearings*, McGraw-Hill Book Company, New York, (1949).